Effect of green infrastructures supported by adaptative solar shading systems on livability in open spaces

Abstract

Lack of thermal comfort in the existing building stock in many warm summer climates and the COVID-19 pandemic have increased residents' temporary occupation of urban open spaces. However, climate change and other effects such as urban heat islands are also negatively affecting the livability of these spaces. Therefore, strategies are needed to improve the thermal conditions in these areas. In this context, the research designs, simulates and assesses an urban green infrastructure supported by an adaptative solar shading system. For this purpose, a public square to be renovated in Seville (Spain) is chosen. After an analysis of the current situation, more vegetation is added. However, trees are not planted fully grown, so their cover is not enough in the short term and an artificial system that protects from the sun by casting shade and that adapts to both their growth and the seasons is included. The urban space is characterized by on-site measurements, proposing four (initial, intermediates and final) scenarios using computational fluid dynamics simulations in an holistic microclimate modelling system. In turn, changes in thermal comfort are analyzed using the COMFA model. Results show that the air and surface temperature are decreased, reducing the number of hours in discomfort by 21% thanks to incorporating the green structure and by 30% due to the vegetation. It can be concluded that the use of these temporary urban prostheses enables urban spaces regenerated with vegetation to be enjoyed without waiting 20 or 30 years for the trees to mature, encouraging people to spend more time outdoors from the start of the intervention.

Keywords:

Urban green infrastructure, open spaces, solar control, adaptive solar shading, thermal comfort, outdoor livability

Acronyms

BHI	Beam (Direct) Horizontal Irradiation
DHI	Diffuse Horizontal Irradiation
COMFA	Comfort Formula
PET	Physiological Equivalent Temperature
PMV	Predicted Mean Vote
NS	Not Specified
NA	Not Applicable
Csa	Mediterranean Hot Summer Climate
UHI	Urban Heat Island
w	Blade Chord
s	Blade Pitch
β	Blade Angle
α	Blade Orientation
BVF	Building View Factor
GVF	Ground View Factor
BMR	Basal Metabolic Rate
CLO	Clothing insulation

1. Introduction

The lack of thermal comfort in the existing building stock in many warm summer climates (Escandón et al., 2019) and the COVID-19 pandemic (Alhusban et al., 2022) have led to an increase in the temporary occupation of urban spaces by residents. Exposure and vulnerability to excessive indoor discomfort (Thomson et al., 2019) require the exploration of different strategies to provide safe outdoor spaces for the population. In addition, the growth of urban areas and the recent public health situation highlight the need to use open spaces for leisure activities (Zabetian and Kheyroddin, 2019). Open spaces in urban environments benefit their occupants (Lai et al., 2019). However, the effects of the climate change can put their health at risk, which is becoming critical at present (Degirmenci et al., 2021). Moreover, global warming in general and the overheating of urban areas in particular have attracted the scientific community's attention for their adverse effects on the population's health (Garshasbi et al., 2020). In this context, taking action on open spaces is essential, especially if this intervention involves mitigation strategies that improve their thermal comfort conditions.

According to the literature, more than 65% of the world's population will be living in urban settings with poor environmental quality by the middle of the twenty-first century (Nations, 2018). This challenge highlights the need to create sustainable open spaces (for instance, cooler spaces in warm climates) within cities to enhance their livability. To this end, mitigation strategies should be used to reduce air and surface temperatures (Mehrotra et al., 2021) and to control solar radiation (Mahmoud, 2011). The present study focuses on designing, simulating and assessing solutions for reducing air and surface temperatures and controlling solar radiation through solar shading.

Solar control strategies in open spaces are based on the use of shade to reduce solar radiation on the areas to be conditioned. Tree shading is one of the most widely used passive strategies for improving thermal and microclimatic conditions (Meili et al., 2021). This type of intervention plays an important role in altering urban areas (Darvish et al., 2021), improving the outdoor microclimate (Fahmy et al., 2020), and enhancing the quality of the outdoor space (El-Bardisy et al., 2016). Indeed, greenery infrastructures, such as parks or high vegetation, and blue infrastructures, such as fountains and ponds, remain some of the most effective measures for cooling urban areas (Degirmenci et al., 2021). In addition, the role of vegetation in urban spaces is not limited to modifying the microclimate, as it also makes them more aesthetically pleasing (El-Bardisy et al., 2016; Lai et al., 2019). Incorporating more greenery infrastructures in urban areas helps to decrease air and surface temperatures (Darvish et al., 2021), mean radiant temperature, humidity, wind speed (Meili et al., 2021) and noise levels (Dimoudi and Nikolopoulou, 2003). However, these benefits depend on the type of vegetation used, its height and the percentage of the area covered by it.

On the other hand, artificial shading is also gaining interest for mitigating the effects of the urban heat island (UHI), as it behaves similarly to vegetation, as will be proven below. For instance, sun sails have traditionally been used for shading streets to improve their thermal comfort levels (Elgheznawy and Eltarabily, 2021). These elements act on the city climate by reducing the solar radiation incident on the treated area. In turn, they reduce the air and surface temperatures, as well as the wind speed, just like their green counterparts. However, their effects on the urban microclimate depend on their optical properties, colour and openness, as well as their spatial distribution, size and layout. In this regard, Table 1 shows research from the literature review on green and artificial shading solutions, highlighting their main features, the type of urban spaces where they were incorporated, the climate in which they were analyzed and the assessment of their energy impact.

93
94

Table 1. Review of shading solutions

Reference	Year	Type of shading solution						Type of study	Zone of study	Type of climate	Impact
		Greenery			Artificial						
		Type of greenery	Mean height (m)	% of area covered	Colour	Mean height	% of area covered				
(Dimoudi and Nikolopoulou, 2003)	2003	Perennial and deciduous	NS	NS	NA	NA	NA	Simulation	Urban space	Hot-summer Mediterranean (Csa)	Decrease of 2ºC in air temperature compared with treeless case in an area of 10x10m. Decrease of up to 3ºC in an area of 18x18m. The type of species does not alter the temperature decrease.
(10.48044/jauf.2013.021)	2013	Perennial and deciduous	4-5	NS	NA	NA	NA	Experimental	Urban Street	Marine west coast (Cfb)	Decrease of 12 to 20 ºC in the surface temperature depending on shade density but less than 1ºC in air temperature.
(Watanabe et al., 2014)	2014	Pergola with plants	NS	90-100	Medium	NS	45-50%	Experimental	University Campus	Humid subtropical (Cfa)	The building shade and pergola shade with plants provided cooler thermal environments with ETU reductions of 16.2 ºC and 18.4 ºC, respectively, compared with sunlight.
(Upreti et al., 2017)	2017	NS	NS	16-30%	NA	NA	NA	Simulation	Urban space	Tropical desert (BWh)	Decrease of 2 to 9ºC in the surface temperature and between 1 and 5ºC in air temperature during the day thanks to the vegetation.
(Kántor et al., 2018)	2018	Perennial and deciduous	9-10	Whole streets	NA	NA	NA	Simulation	School playground	Warm Summer Continental Climate (Dfb)	Mean drop of 1ºC in air temperature surrounding the buildings. Increase in thermal comfort, 5-point drop on PMV scale.
(Kántor et al., 2018)	2018	Perennial	9	NS	Medium	7m	100%	Experimental	Urban space	Warm summer continental (Dfb)	Decrease of up to 10ºC on PET scale, of 1ºC in air temperature and 21ºC in mean radiant temperature on cloudless days with mature trees. A drop of 13ºC on the PET scale, of 27ºC in mean radiant temperature and

											0.4ºC in the air temperature with high sun shading.
(Lee et al., 2018)	2018	Perennial and deciduous	NS	100% of reference point	Medium	NS	100% of reference point	Experimental	Urban space	Warm-summer continental (Dfb)	Better results were achieved with greenery shading than with artificial shading regarding temperatures and level of comfort (according to COMFA analysis).

95

(Kotharkar et al., 2020)	2020	Perennial and deciduous	9.5	25%	NA	NA	NA	Simulation	Urban space	Tropical savanna with dry winter (Aw)	Decrease in air temperature by planting vegetation.
(Fabbri et al., 2020)	2020	Perennial and deciduous trees and bushes	NS	33-54	NA	NA	NA	Simulation	Archaeological site	Humid subtropical (Cfa)	Decrease 2% on PET scale, between 3 and 5ºC in air temperature and 20ºC in surface temperature, due to an increase in area from 33 to 54 m2.
(Peeters et al., 2020)	2020	NS	NS	60-85%	Light-dark	NS	80-100%	Simulation	Urban space	Hot-summer Mediterranean (Csa)	Neutral thermal sensation on PET scale with a percentage covered at least 60% if vegetation or at least 80% if artificial.
(Jia et al., 2021)	2021	NS	0.9-10	NS	NA	NA	NA	Experimental	Urban space	Humid subtropical (Cfa)	An increase of about 20% and 28% in the Green Infrastructure presence case was separately found for concentration levels of particles, compared with the GI-free case.
(Azcarate et al., 2021)	2021	Perennial and deciduous	6-15	24.5-90%	NA	NA	NA	Simulation	Urban space	Temperate oceanic climate (Cfb)	With an average of almost 80% of surface shaded, the Tmrt in the central daylight hours can be reduced to 23ºC. It can be considered an average of 60-70% as a suitable shaded surface target.
(Darvish et al., 2021)	2021	Perennial and deciduous	9	NS	NA	NA	NA	Simulation	Patio between buildings	Cold semi-arid (BSk)	13ºC decrease in mean radiant temperature on the hottest day of the year with the addition of trees.

(Meili et al., 2021)	2021	Perennial and deciduous	3-12	NS	NA	NA	NA	Simulation	Urban space	Tropical rainforest (Af)	Decrease in the universal thermal climate index in a tropical city of at least 3ºC during the day.
(Sabrin et al., 2021)	2021	NS	8	NS	NA	NA	NA	Simulation	Urban space	Humid subtropical (Cfa)	Decrease in the mean radiant temperature of 8ºC and 1.7ºC on PET scale.
(Elgheznawy and Eltarabily, 2021)	2021	NA	NA	NA	Dark	Inclined 3-15m	0-80	Simulation	School playground	Tropical desert (BWh)	Decrease of 1ºC in temperature, 20% on PMV scale, 24% in mean radiant temperature, and of 1ºC on PET scale.
(Nasrollahi et al., 2021)	2021	NA	NA	NA	NS	12m. max.	0-100%	Simulation and experimental	Urban space	Hot semi-arid (BSh)	Decrease in air temperature of 2.2ºC with 100% shade.
(Zeeshan et al., 2022)	2022	NS	NS	Whole street	NA	NA	NA	Simulation and experimental	Urban street	Tropical desert (BWh)	Decrease of 4ºC in the surface temperature and of 1ºC in air temperature.
(Lam et al., 2022)	2022	Decidius	10-25	0-100	Light-Dark with changes in transparency	5	0-50	Simulation	University Campus	Humid subtropical (Cfa)	Artificial shading is a viable alternative to urban greenery when tree planting is impracticable. The main effect of shading devices is the reduction of solar radiation, which subsequently reduces the Tmrt, in contrast to the low reduction in air temperature.

Note: Not specified (NS), Not applicable (NA)

As the table above shows, the most common solution is natural shade provided by vegetation. Compared with artificial shading systems, greenery shading achieves better results in reducing air and surface temperatures, thereby increasing thermal comfort. However, all the research papers in the literature review except (Armson et al., 2013) assess the impact of mature trees many years after planting in the area under consideration. Therefore, temporary or permanent solutions are required, which are adapted to the growth of trees, enabling the objectives to be achieved as soon as the trees are planted, thus making short-term solutions compatible, integrated and harmonized with long-term ones. This gap motivates this study.

In addition, discussing existing and exploring new solutions is not enough. On the contrary, it is necessary to assess the thermal impact they would generate in urban environments (Zhu et al., 2023). This impact should make it possible to quantify the improvement in livability that is generated in open spaces (Georgi and Dimitriou, 2010). Consulted works use outdoor thermal comfort indicators for this purpose (Nasrollahi et al., 2021; Peeters et al., 2020). These comfort indicators are based on the calculation of the physiological response of the external and internal excitations of the human body and the subsequent comparison of the quantitative value with a series of empirical scales that enable judging the level of satisfaction (Kohler and Phillip, 2020). The quantification of these comfort indicators is usually based on measured data and simulation results (Park et al., 2021). These simulations are required for calculating radiant distribution in urban environments or even air movement, as stated by authors such as Garreau et al. (Garreau et al., 2021) or Guo et al. (Guo et al., 2020). However, at the urban level, different tools appear that either partially solve the required needs, as detailed by Zhu et al. (Zhu et al., 2023) in their comprehensive review, or entirely solve them, as proposed by tools such as ENVI-MET (Bruse, 2018). This tool is the most widely used in the literature to simulate urban environments. It solves the radiant characterization in both shortwaves (solar distribution) and long waves as mean radiant temperature, which was evidenced by Nasrollahi et al. (Nasrollahi et al., 2021). These results are easily actionable for calculating thermal or visual comfort indicators (Lam et al., 2022). In addition, the tool's capability facilitates assessing the radiant impact of any solution (any geometry and material) (Unal Cilek and Uslu, 2022). Furthermore, its database for the evaluation of plant solutions must be highlighted, as it contains many plant species with geometric, thermal and aeraulic definitions. This turns it into the leading tool for perspective studies in urban environments for green solutions (Thomas et al., 2023; Yin et al., 2022). For this reason, this paper proposes the use of ENVI-MET from the data measured by a detailed experimental campaign of the thermal excitations of the studied open space and its use by citizens as input data.

The objective of the research is to improve the thermal comfort of open space by means of the design, simulation and assessment of a mitigation strategy that involves the application of an artificial adaptive solar control solution combined with vegetation. In this regard, a real case of a public square to be renovated in the centre of Seville is used. The proposed solution is defined as a green structure, in which trees play a vital role. However, the trees to be planted are small and will take many years to reach mature size. Consequently, in order to improve the thermal comfort in this urban open space since the planting of the vegetation, the incorporation of artificial solar control is studied. This system can be adapted to winter and summer, and its geometry can be modified according to the growth of the trees. This intervention will provide the place with shade until the trees reach the required size so that the bioclimatic behaviour of the urban space will be enhanced from the outset. It can be noted that this urban prosthesis is designed according to the issues presented by the actual area, characterized by on-site measurements. The effect of the integration of solar shading and vegetation is simulated and assessed using ENVI-met, taking into consideration four different scenarios resulting from the growth of the trees.

2. Method

From a methodological point of view, this research is based on a literature review and a case study. The literature review is centred on green and artificial shading solutions for open spaces, whereas the case is explorative. As stated above, the research takes place in a public square in the centre of Seville, which is actually going to be renovated. The results of this study are input data for the renovation of this urban space. The theoretical sampling of a single case study may be straightforward if it is chosen because of being revelatory, exemplary, and/or representing opportunities for gaining research insights (Yin, 2013). While

an experiment isolates the phenomena from its context, the case study emphasizes the rich and real-world context in which it occurs. For the interested reader, Eisenhardt and Graebner (Eisenhardt and Graebner, 2007) provide the keys to build a solid case study. Therefore, this case study has been structured in the following phases:

1. Analysis of the boundary conditions that affect outdoor thermal comfort. For this stage, the traffic on the perimeter, the intensity of use, and the climatic conditions of the square were monitored in detail. Then, the intensity of use was measured with cameras to determine the places of maximum occupation and to characterize the anthropogenic heat. Finally, the climatic data from a climatic station with a record of direct and diffuse radiation and atmospheric radiation were compared with the climatic conditions measured by "on-site" measurements of air temperature and air velocity. In addition, detailed thermographs were performed to confirm the results of the simulation.
2. Design of the proposed solution as an adaptive prosthesis to tree growth, based on the analysis described.
3. Establishment of the indicators and their calculation procedure. For this purpose, the COMFA model is used to assess outdoor comfort. The variables needed for the calculation of the different required heat fluxes are obtained from the simulations of the ENVI-met tool. Finally, the detailed results of these variables and the urban impact of the proposal are shown.

The geographical location, latitude and environment of the city of Seville characterize its climate, with severe warm summer months. Indeed, Seville is the hottest of all the province capitals on the Iberian Peninsula. According to the Köppen-Geiger climate classification, Seville belongs to the Csa category, characterized by warm, dry summers and mild, fairly wet winters (Peel et al., 2007). The daily mean temperature in 2021 was determined from the rural weather station "La Rinconada", which is located outside Seville and does not take into account the UHI effect. However, it can be noted that Seville centre clearly suffers from this effect (Romero Rodríguez et al., 2020). Figure 1 shows that average daily temperatures during the year do not fall below 4ºC in the coldest months, with temperatures between 25 and 30ºC for most of July and August. The high temperatures reached in July and August in Seville result in outdoor spaces hardly being used during these months. For instance, the maximum hourly temperature reached in 2021 was 43.7ºC on 16th August. Furthermore, as can be observed by comparing Figure 1 with Figure 5, the Urban Heat Island Intensity (UHII) is greater during the night, reaching the highest values around 05:00–07:00 h. The results showed a maximum UHII value of 3.1 °C during the evaluation period, which was measured at 22:00 h. However, the highest observed UHII of the fixed temperature sensor occurred at 07:00 h on 20th July, reaching a value of 7.2 °C. Therefore, these conditions result in low-quality outdoor thermal comfort and turn urban environments into hostile territories of low livability unless these comfort conditions would be improved (Stocco et al., 2015).

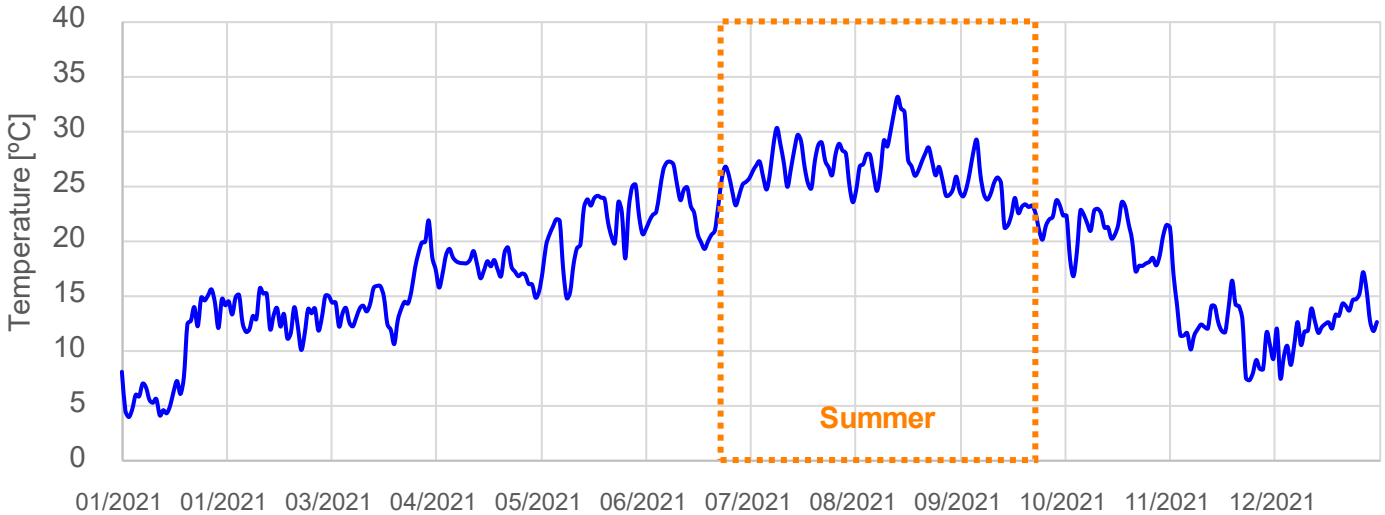

Figure 1. Mean daily temperature from the reference La Rinconada rural weather station (Seville 2021)

The area selected for analysis is a square in Seville city centre (coordinates 37º 24' 13.8" N, 5º58'51.9" W), which is currently going to be renovated. At the height of 13 m above sea level, this square has an area of 612 m^2, mainly covered with paving stones. Figure 2 shows the situation in the square before the renotavion, which is formed at the intersection of three streets. To the east, it borders the narrow street Dr. Jímenez Díaz, which separates it from buildings 15 metres high. To the west, it borders a road with similar characteristics, which separates it from smaller buildings 6 to 9 metres high. To the north, it borders with the Arias Montano primary school. To the south, it borders with Avenida de la Cruz Roja, a street wider than the others and with heavier traffic, which is composed by two roadways with a small traffic island separating them. In addition, the square has very little vegetation. There are eight small trees with a mean height of around 5 metres, featuring only a large Ficus tree in front of the entrance to the school.

Figure 2. Square before renovation

First, as traffic is the primary source of anthropogenic heat affecting the UHI effect of cities where action can be taken (Romero Rodríguez et al., 2020), its intensity in the area was measured with a manual counter. The vehicles circulating over the three streets around the perimeter of the square were numbered during five working days of a week, in the three central hours. A distinction was made between small private cars and larger ones such as buses. Figure 3 shows the number of vehicles measured during the campaign. While the orange columns correspond with heavy vehicles, the blue ones correspond to light vehicles, showing that private cars are mainly responsible for the traffic in the area. In addition, following the distinction between moderate and intense traffic made by Google Maps (Romero Rodríguez et al., 2020), the square is subject to very high traffic density, which reaches its peak at 14.00h, matching the end of the working and school day. This inflow may cause an increase in air temperature, noise and pollution, as indeed was measured later.

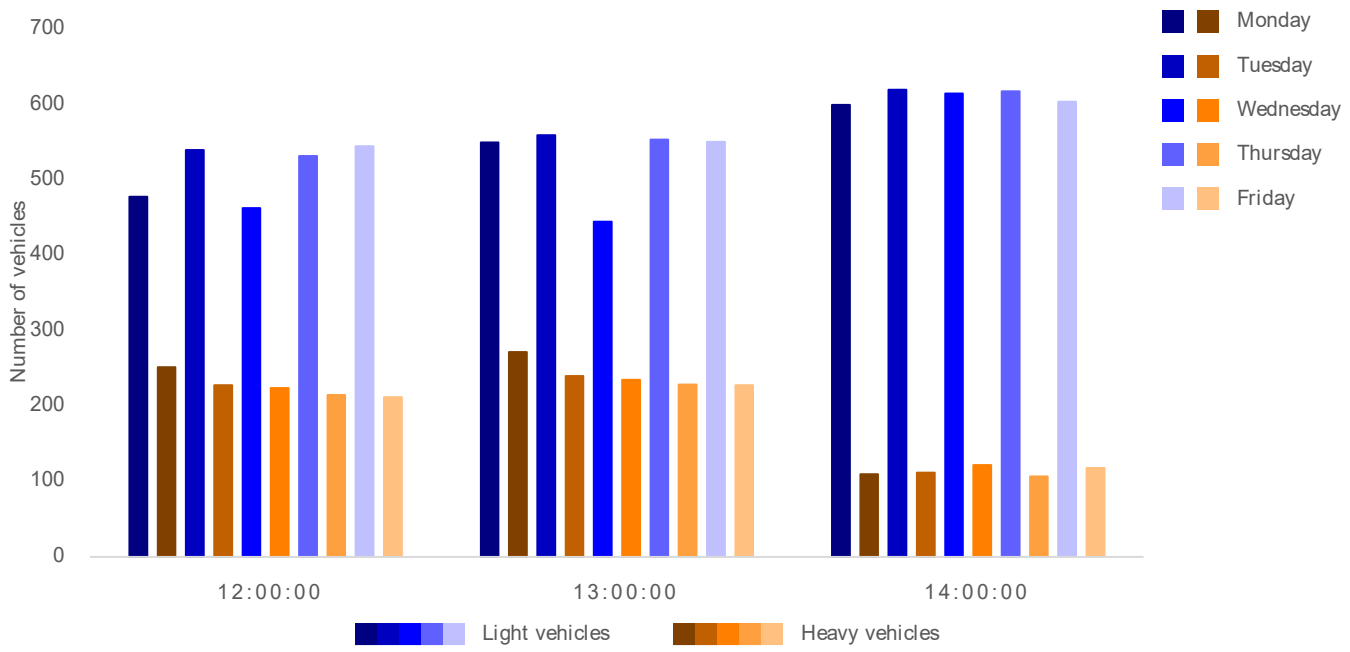

Figure 3. Average hourly vehicle traffic around the square before renovation

Then, to determine how the square is being used before the renovation, a measurement campaign was conducted from April to June 2021, coinciding with the monitoring period that will be described below. To this end, two cameras were placed in the vicinity of the square, as shown in Figure 4, at such an angle to enable the whole square to be visualized. For this purpose, a camouflaged wooden nest was designed to contain the cameras used in the study, which were powered by batteries that were replaced every week. The analysis of the cameras showed that the area did not have a high level of use. Most of the occupants were passing through, staying for a maximum of 10 minutes. The periods of greatest use were at the beginning and end of the morning, coinciding with the start and end of the school day. On such occasions, the number of people increased significantly due to the arrival and departure of pupils to and from school, and the presence of parents and relatives. In the afternoon, there was again a lower peak due to the presence of family members and teachers participating in extra-curricular activities. In relation to staying areas, the most crowed area was the northwest part of the square, corresponding with the entrance and exit of the school. This area with the highest number of walkers and visitors is the choice of the location for the adaptive solution.

Finally, to understand why the square is occupied before the renovation, the initial climate conditions were characterized. To this end, a monitoring campaign was conducted from April to June 2021. Fixed temperature and humidity sensors with five-minute sampling periods and internal memories were installed, ensuring data to be recorded for two months. The sensors selected are the OMEGA OM-92 model, which provide a range of air temperature between -35 ºC and 60 ºC, with an accuracy of 0.2 ºC, and relative humidity between 0 and 100%, with an accuracy of 3%. These sensors were placed in a pair of cylinders of 16 cm high and 6 cm in diameter, perforated on the sides to enable air circulation and fixed with a 15 cm diameter cover to avoid contact with rainwater in case of precipitation (as can be checked in Figure 4, bottom right corner “3 and 4: sensors location”). The covers were painted in dark and medium green colours, making them difficult to detect once in place. However, these were then downloaded to enable recordings in the third month. These sensor devices were placed in two square points, both in the shade, to avoid overheating them. Figure 4 shows where the sensor systems were located, as well as Figure 5 shows their results for a week in May. Temperatures were recorded between 15 and 35 ºC, with even higher temperatures on some days. This example illustrates that temperatures are high even in intermediate months.

Figure 4. Cameras (1 and 2) and sensors (3 and 4) location in square before renovation

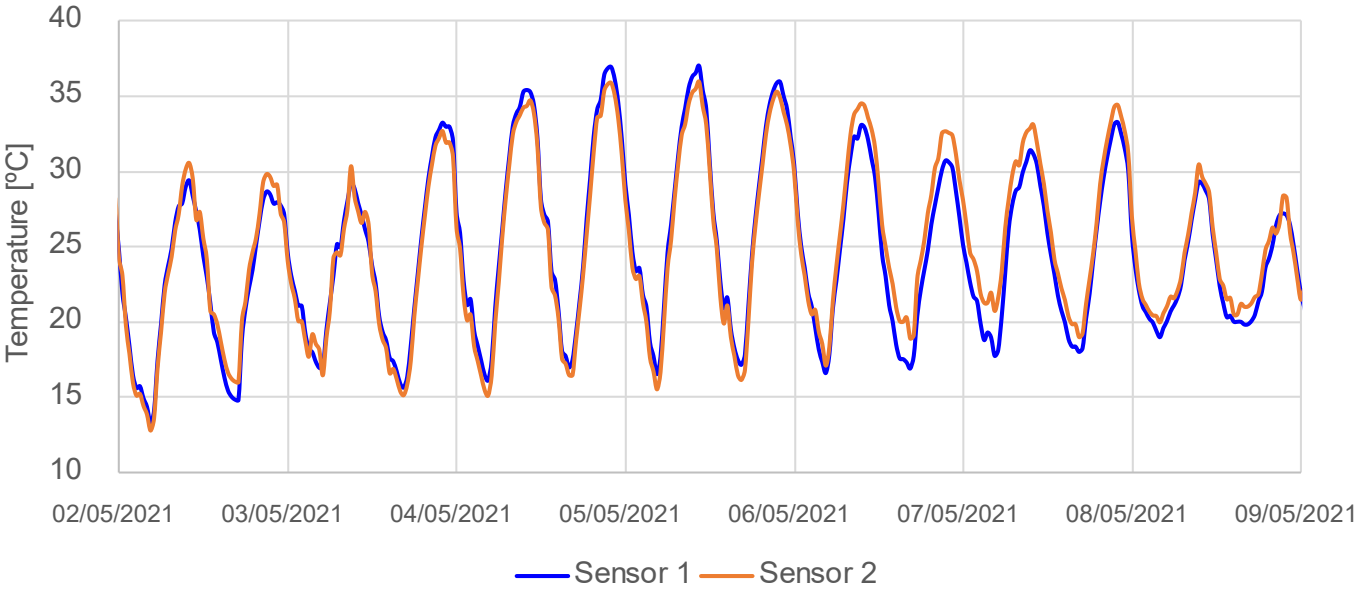

Figure 5. Air temperature during a week in May in square before renovation

In addition to air temperature, the overheating of surfaces has a negative impact on human comfort(Lindberg et al., 2016). Accordingly, the understanding of surface temperatures is an essential part of the sustainable design of urban spaces. The most commonly used techniques are contact thermometers and infrared thermography for measuring these values (Garcia-Nevado et al., 2020). During the campaign, measurements of surface temperatures were also made using a Testo 875i thermal imager over several days at different times. As a result, Figure 6 is an example of the temperature gradient existing in the square before renovation between areas that are in the sun all day and those that are mostly shaded. Thanks to the existing trees, differences of up to 7 ºC were obtained. This is evidence that trees help to reduce the overheating of surfaces and, consequently, of the air. In summary, the high air and surface temperatures reached in the study area, mainly due to the absence of trees, highlighting the need for action in the square

to take advantage of its renewal. This creation of more comfortable spaces, with shaded rest areas that make the place more livable, is the main motivation for introducing a solar shading solution that integrates with the trees.

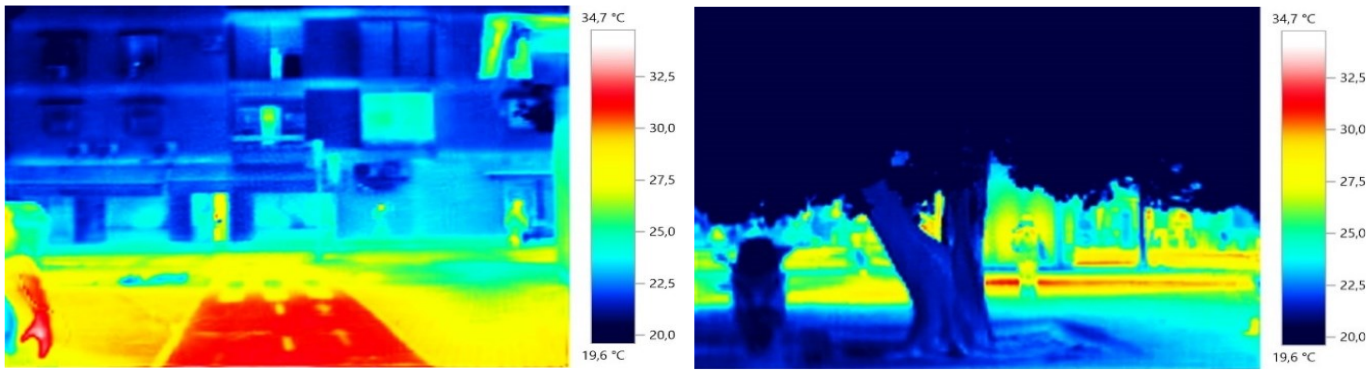

Figure 6. Thermal images of the square before renovation

2.1. Description of the intervention

The intervention proposes to renovate an open space in the centre of the city of Seville that promotes the relationship between its inhabitants and nature. In addition, it will provide a natural, long-lasting shade, with evident benefits for the environment, which in the long term will improve the livability of the urban area. To this end, a study was conducted on how to provide the open space with shade through the greenery created solely by vegetation. To this end, the number of trees in the square will be increased by 300%, adding five new species to produce a green cover.

However, it can be noted that the trees will be planted in their early stages of growth, so during the first years, they cannot provide the desired shade, which is required to improve the thermal comfort of the urban area. However, tree growth is directly related to the thermal conditions of the environment (Takakura et al., 1971). A distinction must be made between fast-growing and slow-growing trees. In this regard, the tree species used in the square are all fast-growing ones, requiring an average of 25 to 35 years to reach mature size. As they will be planted at an average age of 5 years, they will take 20 to 30 years to become fully grown.

Given these restrictions, until the trees reach a size to shade this urban space, an artificial green structure is proposed, which will combine the existing vegetation, the new small trees and the temporary adaptive shading system. This artificial solution must be able to adapt to the growing trees and the seasons of the year, providing shade in summer but letting the sun shine through in winter. The final goal is for nature to prevail and for the prototype to solve the problem while the trees grow. Therefore, according to the tree growth, the intervention can be divided in time into four scenarios, as summarized in Figure 7:

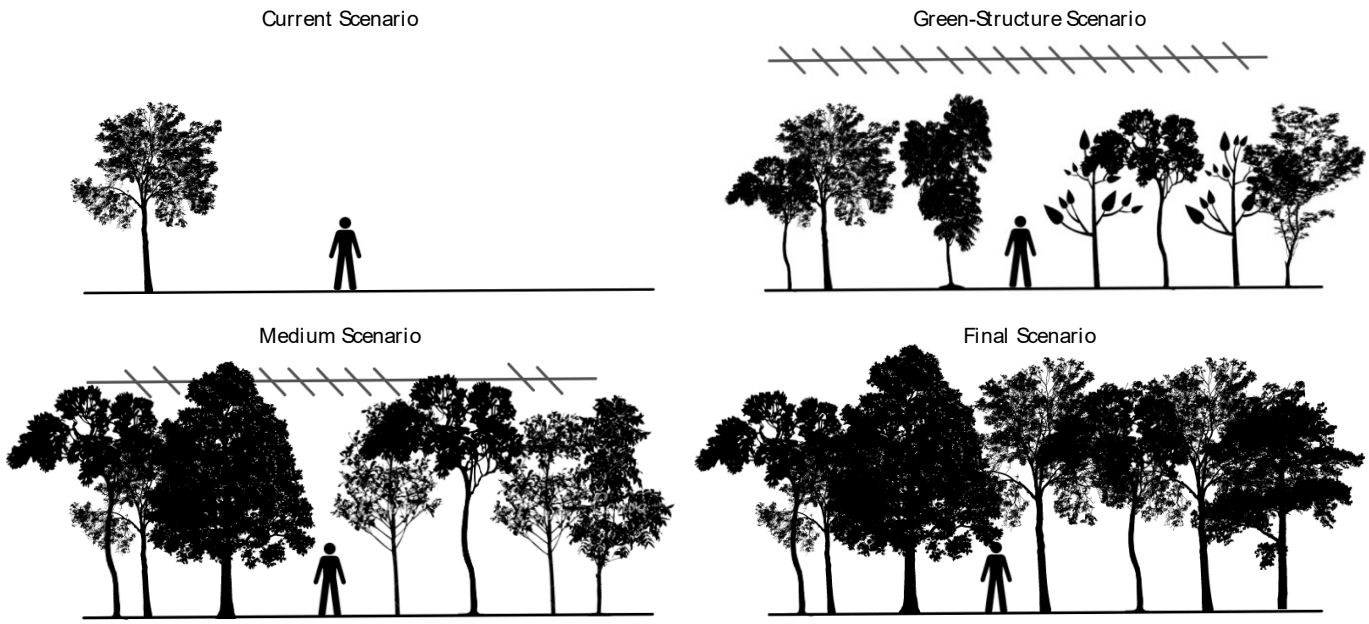

Figure 7. Scenarios proposed for the square before,during and after renovation

1. Current scenario: Only a few trees exist, with no additional element providing shade. Nearly the whole space is in the sun.
2. Green structure scenario: All the new trees are planted in the square, but these are small. Accordingly, the artificial system provides all the shade.
3. Medium scenario: The trees have grown to half their adult size, which enables the artificial system to be partially replaced.
4. Final scenario: The trees are mature and sized enough to provide shade for the whole square. The artificial system is no longer required.

2.1.1. Design of the green structure

The design of the green structure should keep its construction simple and its cost and maintenance low, making it to easy to expand and replicate. Furthermore, when the trees reach maturity and are not needed in the square, the anchoring system should enable the complete structure to be dismantled easily for use elsewhere if required. Therefore, the green structure assembly consisted of individual structures that can be linked together, providing continuous shade while creating visually appealing layouts. These individual structures were designed to resemble in shape and size the trees that they are temporarily replacing, essentially becoming an artificial tree. Their height was consequently defined according to the average height of the different tree species selected. This means that each structure was designed with a height of 5 metres. The shape of each structure resembled the round top of a tree. However, to facilitate modularity and repeatability of composition, as well as assembly and connections between them, these structures were designed with a hexagonal shape, which can be divided into 6 equilateral triangles. This configuration provides the triangles can be placed in different positions depending on the hours when protection is required. Moreover, as an urban prosthesis, it is possible to adapt its shape to the growth of the trees by progressively removing the triangles that compose the structure. The diameter of each hexagon was determined to be 6 metres to reduce the number of individual structures without exceeding dimensions that increase their mechanical complexity. In turn, each hexagon consisted of six equilateral triangles with sides measuring 3 metres. Figure 8 shows the design of each individual structure and how it can be partially disassembled.

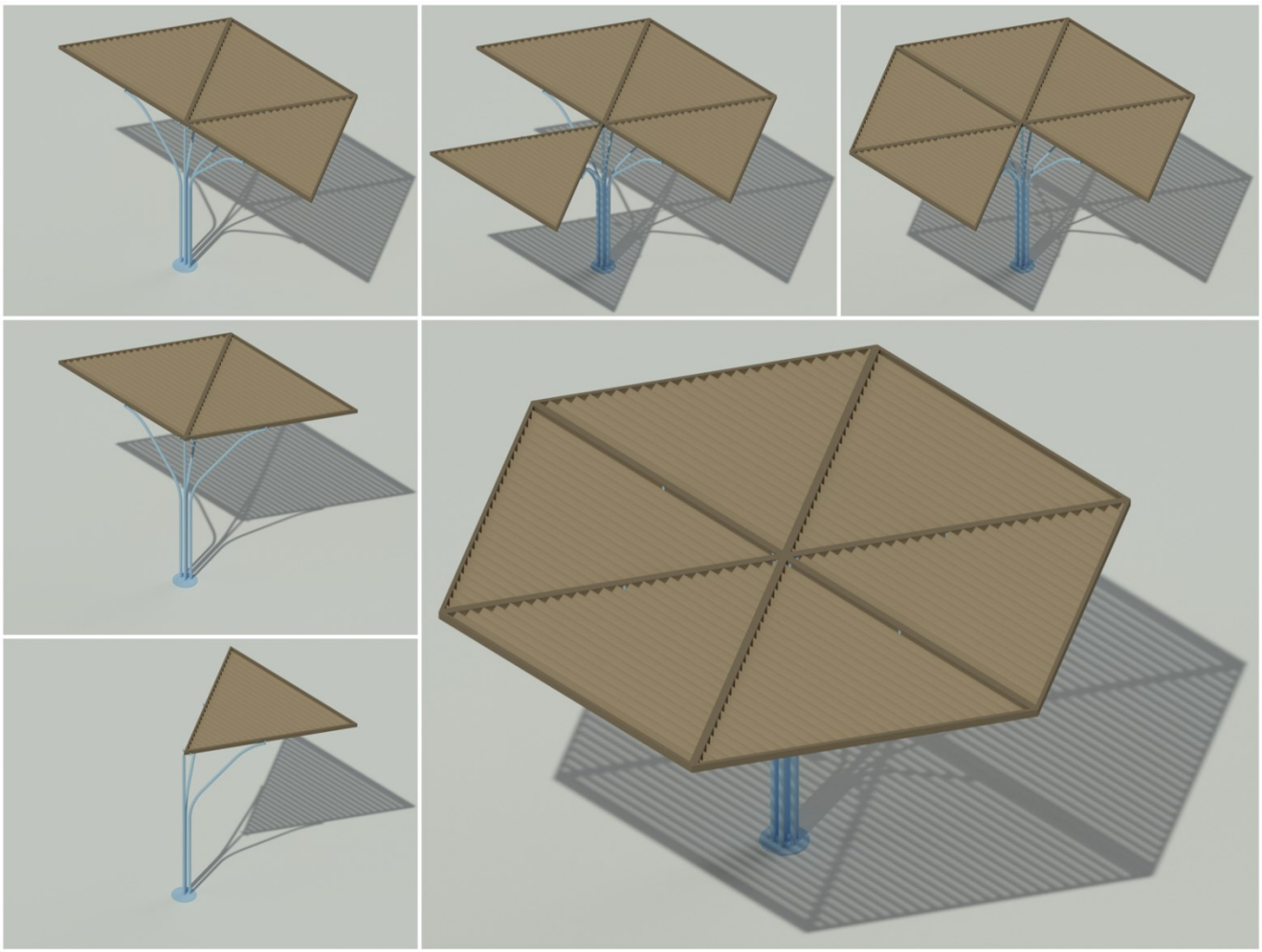

Figure 8. Composition of the breakdown of a green structure element

One of the main features of each element of the green structure was the option of modifying its geometry. In the short term, It can be modified according to the season of the year. Their parts can be removed in the winter to let in more solar radiation if this is necessary. In the summer months, the modules removed can be put back to achieve the shading required in the urban area. In this context, to improve the thermal comfort in the area during the whole year, dealing with radiation played an important role. Accordingly, each triangular module in the green structure should enable radiation during the winter months but block it in summer. This was achieved by using slats as the main shading element. The layout of the slats is defined by their orientation (α), inclination (β), width (*w)* and separation (*s*), as shown in Figure 9. In the long term, the shading system can be adapted to the growth of the trees, permanently eliminating the triangular modules when they grow to the size required to cover the open space. The permanently removed modules could be used in other locations in the city of Seville. This is possible because each triangular module is independent of the others and can be removed to comply with both purposes.

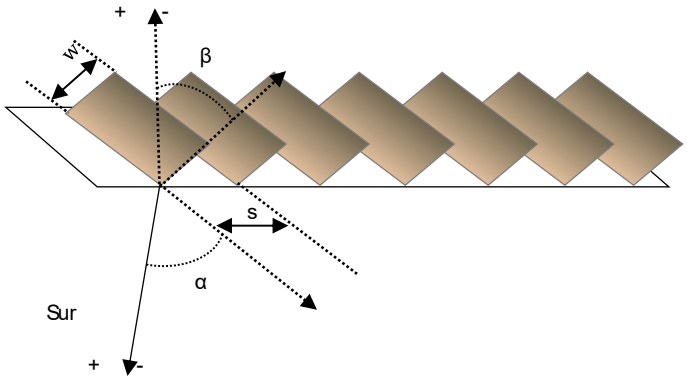

Figure 9. Scheme of the slats in the green structure

Each slat has a thickness of 0.25 cm and a width of 10 cm (w). Slats are made with conventional Bambú (*Phyllostachys aurea*). This material presents these thermal properties: thermal conductivity 0.04 W/mK, specific heat 2.29 kJ/kg·K and density 600 kg/m^3. In addition, the slats were painted in a light colour, with a highly reflective paint (0.95). To determine the optimal orientation (α), inclination (β) and separation (s) of the slats that achieved a significant reduction in the direct radiation on the urban area, an analysis was performed during 8 hours per day (13:00-20:00, GMT+2) on different summer days. The study was conducted in three steps, analyzing the direct and diffuse radiation passing through the slats, as compiled in Figure 10. This study was done by the Tonatiuh simulation software (Blanco et al., 2021, 2005; Jafrancesco et al., 2018; Montenon et al., 2022). This tool implements a Monte Carlo ray tracing algorithm, which enables to analyze the solar incident in any geometry and material. It is commonly used in the literature to study solar effects (Duan et al., 2020). First, for one day and inclination, the influence of orientation and separation was studied. Then, after defining the orientation that provided the best results for direct radiation, the effect of the inclination was analyzed, as well as the separation. Finally, knowing which geometry reduced the direct radiation the most for a single day, calculations were performed for the same day of each summer month in order to confirm the optimal geometry. Moreover, the values used for radiation and the sun position were obtained from a typical year in Seville. The sign convention used in the solar azimuth angle was 0º from the south, positive to the east and negative to the west.

In step 1, a constant inclination was maintained over the normal (β) of −45º for 15th June, with a south-southwest and west-southwest orientation (α=−15º and α=−75º respectively) for a separation of 5, 10 and 15 cm. The results showed that the fraction of direct solar radiation reaching the square was null with a separation of 5 centimetres in both orientations. However, it increased for both orientations as the separation between the slats became greater. This suggested that the separation of 15 cm would not achieve the desired reduction in solar radiation and was therefore rejected. Observing the orientation effect for the urban area, the south-southwest orientation presented higher direct solar radiation fraction values in a more significant number of hours. Therefore, the optimal orientation to be selected was the west-southwest one, rejecting the south-southwest orientation. Having determined the optimal orientation, the slat separation was analyzed according to the inclination. The inclinations were −45º, −50º and −55º for the same typical day. At higher inclination angles, the fraction of direct solar radiation passing through the shading elements decreased. At a separation of 5 centimetres, the radiation was completely blocked again. At 10 cm, although not nullified in all hours, the reduction was also substantial. However, a separation of 5 cm would result in a considerable increase in the number of slats and, consequently, the cost of the green structure. For this reason, the optimal separation chosen was 10 cm and the inclination was −55º. To sum up, the geometry selected was established with slats with a width of 10 cm (*w*), a separation of 10 cm (*s*), with an inclination angle over normal of −55º (*β)* and a west-southwest orientation of −75º (α). To determine the effect of the chosen geometry during the summer months and check that it works correctly, the solar study was performed for the 15th day of each month from June to September for a typical climate year for Seville during the eight hours mentioned above.

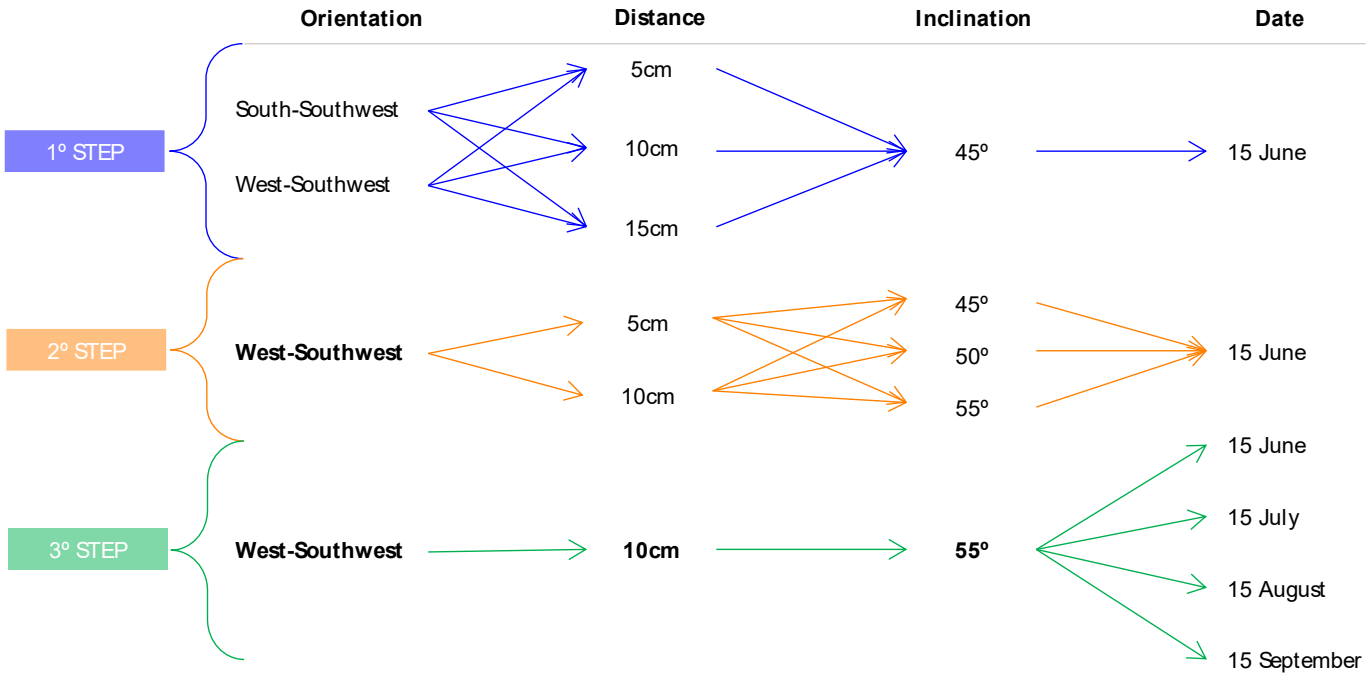

Figure 10. Solar optimization study

As Table 2 shows, the direct radiation was nullified for every hour after 16.00 h, a phenomenon repeated on every day studied. Table 2 shows the simulation results of the solution in different solar positions. The main result is transmissivity, which is calculated as the comparison between the direct or diffuse radiation on the ground and the direct or diffuse radiation of the sun. In addition, only diffuse radiation was transmitted, reducing the radiation's negative effects on the outdoor environment. Although the direct radiation was not entirely nullified during the beginning of the afternoon, it was considerably reduced. In summary, the adaptive artificial shading can substantially decrease solar radiation amount. This will lead to lower surface and air temperatures, improving the thermal comfort and livability of the urban space.

Table 2. Results from 15th July

15th July | α = −75º | β= −55º | s= 10 cm | w= 10 cm						
Hour GMT +2	Azimuth	Solar height	BHI [W/m^2]	DHI [W/m^2]	Transmissivity direct/direct	Transmissivity diffuse/diffuse
13	56.90	64.93	798.00	108.00	0.22	0.30
14	23.99	72.82	867.00	100.00	0.12	0.30
15	− 24.57	72.75	867.00	100.00	0.03	0.30
16	− 57.15	64.79	798.00	108.00	0.00	0.30
17	− 74.54	53.89	672.00	120.00	0.00	0.30
18	− 85.92	42.15	510.00	127.00	0.00	0.30
19	− 94.97	30.23	336.00	122.00	0.00	0.30
20	− 103.28	18.50	174.00	98.00	0.00	0.30

2.1.2. Integration of the designed solution

For the greenery shading strategy to achieve the desired cooling benefits, it is essential to place and dispose of the trees correctly (Elgheznawy and Eltarabily, 2021). The species used were selected according to their height, leaf density and seasonal behaviour. The selection included deciduous trees, which encouraged radiation to enter during winter, and perennials, which ensured shade during the summer. Due to the sun's path in the summer months, the group of trees is in such a position that the whole pedestrian square will be in the shade once they reach adult size.

Table 3 shows the species of trees selected, distinguishing between the existing trees and the new ones to be planted, as well as the expected dimensions in each scenario of the study. The trees to be planted should measure 2.5 m from the ground to the bottom of the crown, as well as the distance to the top of the crown was considered to be 1.5 m, according to the Master Plan for Urban Trees of the city of Seville. The trees

were considered to have an average height of 4 m. Also, the Master Plan for Urban Trees of the city *"seeks to promote the generation of ecosystem services through the promotion of trees considering the use of plants with heritage and cultural value, contributing to the dissemination of their benefits to society. For this, the city rulers have a list of species that they consider acts for their integration into the urban environment. The eligibility criteria of these species are based on the following indicators: water consumption, root growth, mechanical resistance to the effects of the wind and maintenance needs (pruning, generated dirt and chemical treatments)."* On the basis of these conditions, the City Garden Service proposed a set of species for integration into this new green area. The choice of the number of trees and their positioning has been analyzed through the simulations presented here and a collaborative work process with a group of citizens elected as district representatives. This group of citizens voted for the solution that aesthetically and functionally seemed to be the best.

Table 3. Trees used in the square renovation

Number	Species (Latin name)	Condition	Green Structure Scenario Dimensions (Height-Radius)	Medium Scenario Dimensions (Height-Radius)	Final Scenario Dimensions (Height-Radius)
83	Citrus x Aurantium	Existing	5-2	5-2	5-2
84	Citrus x Aurantium	Existing	5-2	5-2	5-2
85	Citrus x Aurantium	Existing	5-2	5-2	5-2
86	Citrus x Aurantium	Existing	5-2	5-2	5-2
87	Citrus x Aurantium	Existing	5-2	5-2	5-2
89	Platanus x Acerofilia	Existing	15-4.5	15-4.5	15-4.5
90	Ficus Benjamina	Existing	9-11	9-11	9-11
91	Platanus x Acerofilia	Existing	15-4.5	15-4.5	15-4.5
92	Platanus x Acerofilia	Existing	15-4.5	15-4.5	15-4.5
N90	Celtis Australis	New	4-2	5.5-6	12-13
N91	Celtis Australis	New	4-2	5.5-6	12-13
N92	Celtis Australis	New	4-2	5.5-6	12-13
N93	Celtis Australis	New	4-2	5.5-6	12-13
N94	Celtis Australis	New	4-2	5.5-6	12-13
N95	Syagrus Romanzoffiana	New	4-2	10-4	15-7
N96	Syagrus Romanzoffiana	New	4-2	10-4	15-7
N97	Syagrus Romanzoffiana	New	4-2	10-4	15-7
N98	Syagrus Romanzoffiana	New	4-2	10-4	15-7
N103	Paulownia	New	4-2	7-4	12-8
N105	Paulownia	New	4-2	7-4	12-8
N106	Paulownia	New	4-2	7-4	12-8
N108	Paulownia	New	4-2	7-4	12-8
N120	Cercis Siliquastrum	New	4-2	7-3.5	8-6
N121	Cercis Siliquastrum	New	4-2	7-3.5	8-6
N122	Cercis Siliquastrum	New	4-2	7-3.5	8-6
N123	Cercis Siliquastrum	New	4-2	7-3.5	8-6
N126	Albizia Julibrissin	New	4-2	7-3.5	8-6
N130	Cercis Siliquastrum	New	4-2	7-3.5	8-6
N133	Albizia Julibrissin	New	4-2	7-3.5	8-6
N136	Albizia Julibrissin	New	4-2	7-3.5	8-6
N137	Albizia Julibrissin	New	4-2	7-3.5	8-6
N139	Albizia Julibrissin	New	4-2	7-3.5	8-6

Location of each tree is shown in Figure 11a. Each circumference is the diameter of the crown when fully grown, proving that the vegetation will shade the entire square once it reaches maturity. The location of the artificial shading was decided according to the new boundary, the use of the space and the growth of the trees. As a result, the proposed design was located in the southwest part of the square, as shown in Figure

11b. Knowing the vegetation used and the location of the green structure, the impact on the thermal quality of the space was assessed for the four scenarios using the ENVI-Met software.

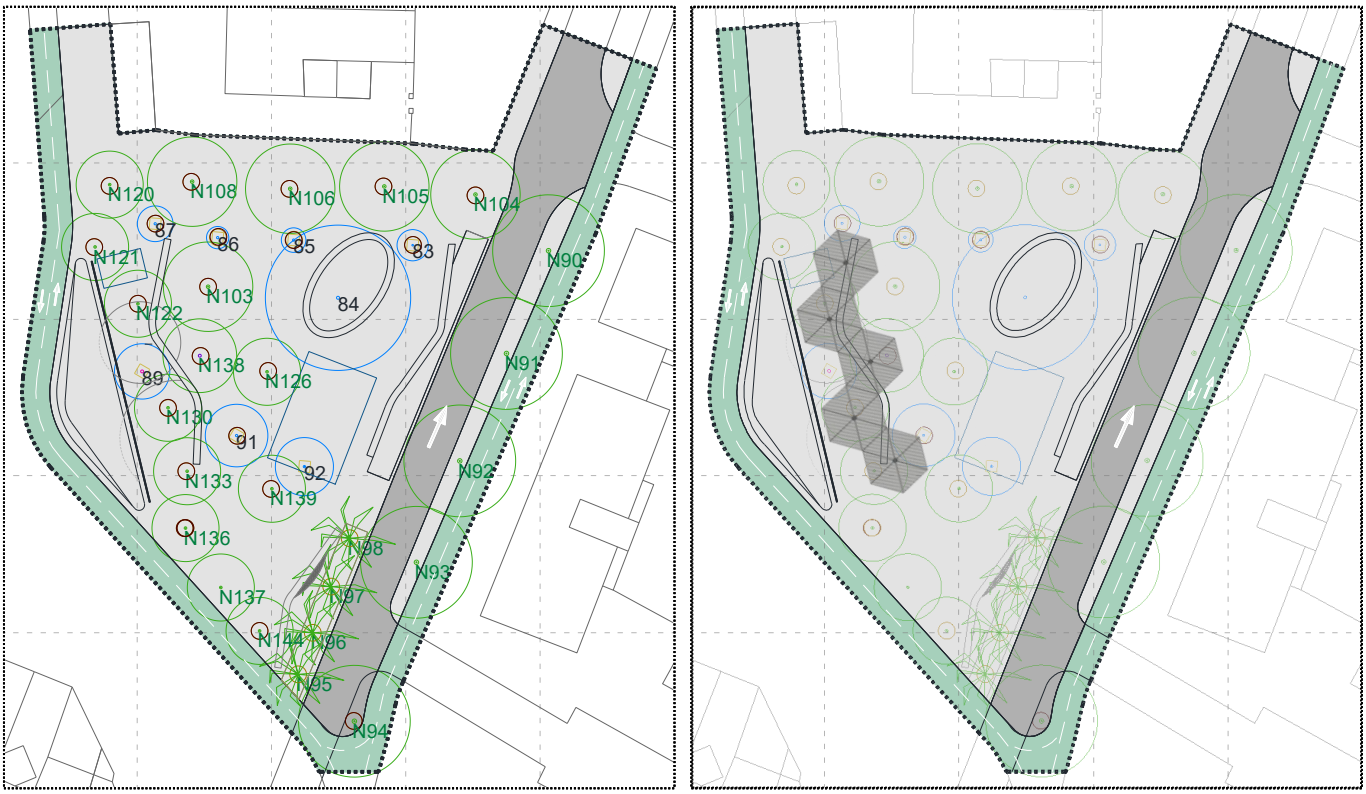

Figure 11. Distribution of the trees (1a) and location of the artificial shading in the square (2b)

2.2. Impact Assessment

2.2.1. Simulation of the urban microclimate using ENVI-Met software

The four scenarios studied were simulated following the ENVI-met microscale number model to assess the impact of the proposed mitigation strategy. The measured data from the initial situation is used as climatic excitations for all simulations. These simulations evaluate the proposed solution's effect and its ability to hybridize with the desired vegetation. The ENVI-met software is a holistic microclimate modelling system in which all the different elements of the city landscape interact ("ENVI-met - Decode urban nature with ENVI-met software," n.d.).This software addresses the interaction between climate parameters, vegetation, surfaces, ground and buildings in the outdoor environment. ENVI-met uses a 3D model consisting of a certain number of grid cells that make it possible to understand three-dimensional wind changes, turbulence, air temperature and humidity, radiation flow, and pollutant dispersion (Chatzinikolaou et al., 2018). The results obtained using ENVI-met simulations have been validated with actual measurements in numerous studies (Elnabawi et al., 2015; Sharmin and Steemers, 2016, 2015).

2.2.2. Model

The geometry of the square under study was defined using the Spaces tool from the ENVI-met software. This converted the actual area into a grid of equal cells measuring 1×1×1 m. The vertical grid had a height of 40 m, doubling the maximum height of the trees, because ENVI-met leaves at least twice the existing maximum height empty, as summarized in Table 4. The resolution of the vertical grid followed the same dimensions as the rest, this being 1 metre, so the grid of the model totalled 60×70×40 m. The vertical grid played an essential role in the simulation of the tool, so it was essential to define the generation method to be followed. In this case study, the choice was made not to use the telescoping function (refining the resolution of the grid near the floor), so all the cells of the vertical grid presented the same dimensions. This resulted in longer simulation times but ensured that the upper areas of the grid were correctly calculated.

Table 4. Definition of the model domain

Latitude (deg, +N,-S)	37.24
Longitude (deg, -W,+E)	-5.58
Reference Time Zone	GMT +2
Model Dimensions (m)	60×70×40
Size of grid cell (m)	1×1×1
Method of vertical grid generation	Telescoping 0%

The climate data used were those in the ENVI-met database. To achieve more precise results in the simulation calculations, these were performed for specific days for which the Simple Forcing option was used. It meant that the temperature and humidity values were forced on the lateral boundaries of the model using the Forced Lateral Boundary Conditions configuration. The simulations were performed for two seasons of the year. The target was to compare the improvement in the conditions in times with high temperatures, namely the summer, and times with intermediate temperatures. To this end, the days chosen were 15th April 2021 and 15th July 2021, the latter being one of the hottest days of 2021. The starting values to simulate for each time (representative day) of the year are shown in Table 5. Simulated hours were from mid-morning to early evening (11:00-19:00 GMT+2).

Table 5. Initial meteorological conditions for simulations

	Summer	Spring
Wind speed measured in 10 m height (m/s)	3	2.5
Wind direction (deg)	225	225
Min. temperature of atmosphere (ºC)	12	5
Max. temperature of atmosphere (ºC)	25	14
Min. relative humidity in 2 m (%)	30	50
Max. relative humidity in 2 m (%)	69	70

2.2.3. Vegetation

To incorporate the vegetation into the model, the ENVI-met database (Albero) was used, which includes over 30 species worldwide, differentiating between deciduous and perennial species. It also provides data for each kind of albedo and shortwave transmissivity, in addition to depth and diameter of roots, which affect the water absorption of each tree. Species from the database were used to model the trees which will be planted in the intervention. However, the dimensions were modified in each scenario while maintaining the characteristics of the species. Table 6 shows the albedo and transmissivity values for each species included.

Table 6. Albedo and transmissivity values of the tree species introduced in ENVI-met

Species (Latin name)	Albedo	Transmissivity
Citrus x Aurantium *	0.4	0.3
Platanus x Acerofilia *	0.18	0.3
Ficus Benjamina *	0.18	0.3
Celtis Australis **	0.18	0.3
Syagrus Romanzoffiana **	0.18	0.3
Paulownia **	0.60	0.3
Cercis Siliquastrum **	0.60	0.3
Albizia Julibrissin **	0.60	0.3

Note: Existing trees (*), New trees to be planted (**)

Figure 12 shows the geometric model that was created following the layout of the vegetation and considering its dimensions and the location of the green structure in the scenarios in which it was used. The surfaces used were granite paving stone for the square and asphalt for the surrounding streets. Its respective

albedos were 0.4 and 0.2, both with emissivity values of 0.9. The green structure was modelled with the Single Wall function, using a material with a transmissivity of 0.4 in order to simulate the behaviour of the slats.

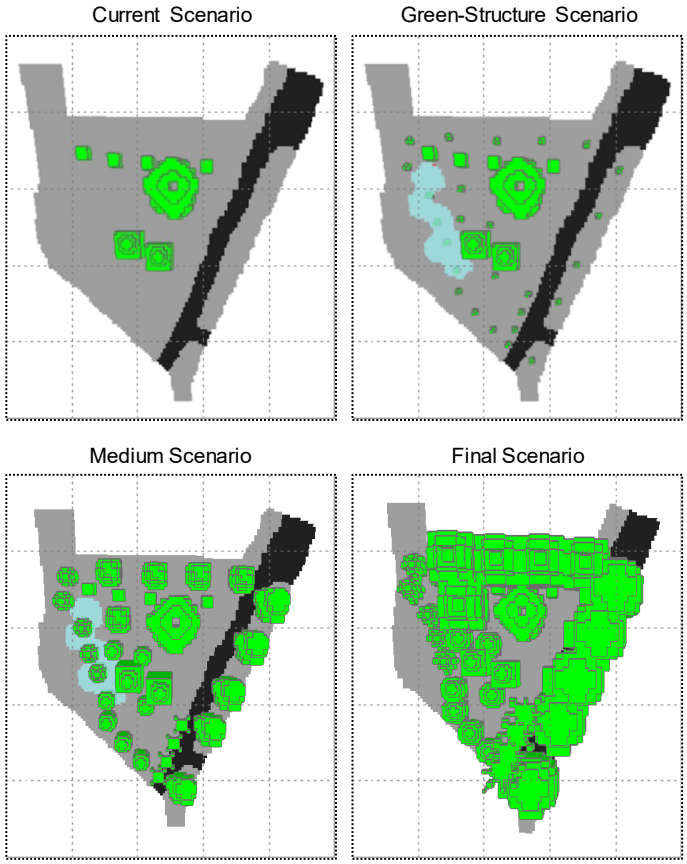

Figure 12. ENVI-met models used for each scenario

2.2.4. Comfort assessment

Thermal comfort is the indicator that was chosen to assess the impact on the urban space. To do this, the results obtained from the data measured before the intervention were compared with the simulation results of the different improvement scenarios achieved by the proposed solutions. This section defines the mathematical formulation of the outdoor thermal comfort indicator, its relationship with the simulated and measured data, and the expected values to evaluate it.

In most outdoor thermal comfort studies, a purely physiological model has been used, involving a mathematical model of the thermoregulatory system employed for calculating the thermal comfort conditions, whereas the subjective responses (thermal sensation) are taken into account by the use of the standardised scale for each indicator. There are two main indicators: PET and COMFA. They are the most used in the literature. PET is widely used indoors and outdoors. There are many works in this line for interior spaces (Ozarisoy and Altan, 2021), but the number of publications is scarcer in the case of exteriors. However, the standardized PET evaluation ranges are of low applicability for hot climates. Li et al. (Li and Liu, 2020) review less warm climatic zones in summer than in the Mediterranean region, but with an important conclusion: the extension of the comfort band generates great possibilities in the future to design strategies to improve the habitability of cities. That is why a previous study would have to be performed to determine the valid acceptability range for hot climates, considering the thermal sensation of citizens in hot climates. On the contrary, there are many works applying COMFA in hot climates, which conclude that values of heat load lower than 100 W/m^2 can be considered acceptable (Sánchez Ramos et al., 2022).

Apart from determining the results achieved in terms of thermal conditions, it is of particular interest to know whether thermal comfort is improved for the occupants of the square. Thermal comfort is an individual response expressing the individual level of satisfaction with the thermal conditions of the environment (ASHRAE, 2017a). This combines the physiological and psychological responses of the

human being, although different connotations in indoor and outdoor spaces must be considered (Höppe, 2002). On the one hand, the physiological response was analyzed using a thermal balance of the human body (Nikolopoulou et al., 2001). This thermal balance is expressed according to Equation 1 (Pearlmutter et al., 2014):

$$\Delta S = (M - W) \pm (C + R) - E \quad (1)$$

Where ΔS [W/m^2] is the energy variation in the body; M is the heat generated by the metabolism [W/m^2]; W [W/m^2], mechanical work, is heat consumption due to the activity being performed; $(C + R)$ [W/m^2] is the convective and radiative exchange with the environment; and E [W/m^2] is the heat loss due to sweating. All the above variables were defined according to the heat transfer coefficient of a person (Du Bois and Du Bois, 1989). In addition, the variables were quantified in detail (ASHRAE, 2017b). For this study, acceptable thermal comfort conditions were considered for outdoor environments (Pearlmutter et al., 2014). The mechanical work value (W) was nullified, and an M value of 2.5 met (116.3 W/m^2) was taken, which is equivalent to a mean activity level between light (2 met) and moderate (3 met). It can be noted that light activity refers to people at rest or walking slowly, while moderate activity refers to people walking at 1.3 m/s.

On the other hand, the psychological response was combined with the physiological one by obtaining experimental relationships (Nikolopoulou and Steemers, 2003). In this regard, there are thermal comfort models and different indices that make its assessment feasible (Coccolo et al., 2016). This study distinguished between three categories of thermal comfort: thermal indices, empirical indices and indices based on linear equations. The indicator used was the one proposed in the COMFA model, formulated by (Brown and Gillespie, 1986) and later reformulated as COMFA+ by (Angelotti et al., 2007). This update added the impact of urban shapes on the thermal load, using the BFV and GVF factors, and proposing the calculation of these parameters using simulation tools. Moreover, the COMFA model proposes a scale based on five levels, as summarized in Table 7. The usefulness (Kenny et al., 2009a, 2009b) and validity (Vanos et al., 2012) of this indicator has been widely documented in the literature. Among methods and tools to calculate outdoor comfort, ENVI-met provides good results for exchanging short and long wavelengths in all directions (Johansson et al., 2014).

Table 7. Levels of comfort

Level	1	2	3	4	5
Heat load Q (W/m^2)	> 150	50 - 150	−50 - 50	50 - −150	< −150
Consideration	Very hot	Preferably cooler	Comfort	Preferably warmer	Very cold

The heat load indicator, Q [W/m^2], is defined as the heat load that the body needs to gain (in winter) or lose (in summer) to maintain its comfort zone. This indicator belongs to the group of direct indicators, as it can be calculated using a basic measurement of the environmental conditions (Epstein and Moran, 2006). This can be defined according to Equation 2:

$$Q = (M - W) \pm (C + R)_{REQ} - E_{REQ} \quad (2)$$

Where $(C + R)_{REQ}$ are still the convective and radiative heat flows exchanged with the person, but taking a required skin temperature T_{SK-REQ} to reach outdoor comfort conditions, according to the ISO 7933 standard (Standard, 2004). In addition, E_{REQ} refers to the perspiration required by the body, as defined in the ISO 7933 standard (Standard, 2004). Both terms are defined in Equations 3 and 4:

$$T_{SK-REQ} = 35.7 - 0.0274 \cdot (M - W) \quad (3)$$

$$E_{REQ} = 0.42 \cdot (M - W - 58.15) \quad (4)$$

The literature review and the establishment of an indicator within a specific range has proven that, in order to ensure thermal comfort (Rupp et al., 2015), skin temperature and perspiration levels must be within certain values (ISO, 2017). The defined temperature and required perspiration according to the above standard would comply with the expressed restrictions. They would be aligned with other standards applied to outdoor thermal comfort, such as the ASHRAE 55 and ISO 7730 standards (ISO, 2005).

For the comfort analysis performed in this study, the average height of a person was taken as 1.65 metres. According to the ASHRAE classification, the BMR values were taken as 2.5 (116.3 W/m^2) in each case, as stated above (ASHRAE, 2017c). Different values were taken for the summer and spring for the CLO values. For the summer day, a CLO value of 0.36 was taken, corresponding to 'walking shorts, short-sleeve shirt', while for the spring day, the value used was 0.57, corresponding to 'trousers, short-sleeve skirt', following the ASHRAE classification (ASHRAE, 2017c). The climate data were used in the ENVI-met simulations for the same days to establish the same conditions in both analyses. The comfort of a person occupying the north-west part of the square was assessed under three conditions: without shade (before renovation), under the artificial solar shade (2 scenarios during renovation) and, finally, under natural shade (after renovation).

The weather station provides to know direct and diffuse radiation, as well as the atmospheric radiation and the effective temperature of the sky, thanks to its pyrgeometer. In addition, an anemometer was included to determine the air speed in the occupied area in the intervention area. These data were recorded from February 2021 to November 2021, and then used in ENVI-met to perform the simulations with the specific microclimatic conditions of the area characterized for each simulation. These conditions refer to the current situation before the renovation. ENVI-met calculated the resulting temperatures in pavements, walls, trees, air, etc... in such a way that the comfort conditions can be characterized according to the explained procedure. For this purpose, the Leonardo module of ENVI-met was used to obtain the values of all the required variables.

3. Results

The results obtained can be divided into those relating to the environmental changes in terms of air temperature, incident radiation and surface temperatures and those relating to changes in thermal comfort. The Panoply Data Viewer software (NASA, 2022) was used to display the results, highlighting the study area with dotted lines.

3.1. Environmental variables

3.1.1. Air temperature

After performing the simulation, the air temperature in the square at the height of 1.5 m was obtained to determine the conditions at an average height for the occupants, both in summer and spring and at different times of the day. Figure 13a shows the air temperature for the four scenarios analyzed on 15th July at midday. It can be noted that the incorporation of the vegetation in the final scenario decreased the temperature by around 1ºC compared with the current scenario in the area with the highest concentration of trees. ENVI-met software performs a numerical calculation on a surface and volumetric mesh. Surface temperature values are strongly influenced by incident solar radiation, hence the shading effect. In turn, the air temperature due to the convective effect with that surface temperature, will have overheating due to the surface since the prevailing wind direction causes the wind to pass through the cover in the first place. Moreover, there was a decrease in the negative effect of hot surfaces, such as the tarmac on the roads around the square. In the green structure scenario, a reduction in temperature was achieved by including artificial solar shading, although the temperature drop is small. Regarding the medium scenario, in which the vegetation is generally not very dense, the decrease in temperature was lower than that obtained in the final scenario, with a difference compared with the current scenario of 0.5 ºC. The effect was similar at 18:00 on the same day, as shown in Figure 13b. At this time, the temperature in the square was higher due to heat building up during the day, reaching nearly 35 ºC in the surrounding area. However, inside the square, a temperature difference of 0.8 ºC was observed between the current and final scenarios. In contrast, in April,

633 the air temperature was lower in the whole square, as shown in Figure 13c. For 15th April at noon, a 1 ºC
634 decrease in air temperature was again achieved between the extreme scenarios. The slight reduction in air
635 temperature in the green structure scenario, where the vegetation is minimal, and there is only artificial
636 shade, confirmed the importance of vegetation in reducing the temperature.

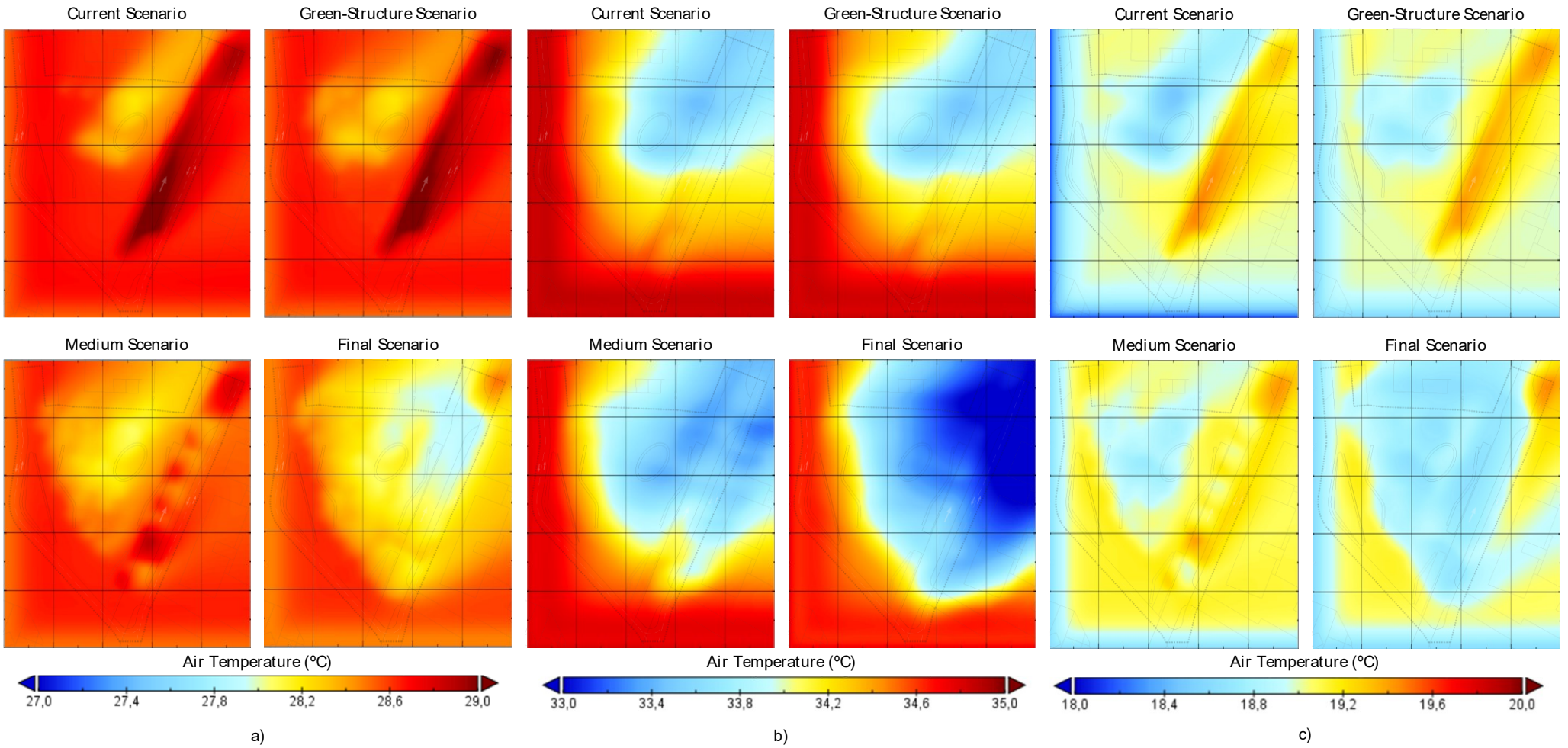

Figure 13. Air temperatures in the four scenarios for 15th July at 12:00 (left), at 18:00 (centre) and for 15th April at 12:00 (right)

In addition, Figure 14 shows the evolution of the average air temperature (Figure 14a) and the mean radiant temperature (Figure 14b) at 1.5 metres above the ground for the whole square throughout 15th July in the four scenarios. The difference in air temperatures of 0.5ºC between the current and final scenarios remained practically constant. However, the mean radiant temperature difference (as can be checked in Figure 14b) shows a beneficial effect for pedestrians. In the current scenario, a person located in the centre of the area would be able to see the sky. In this context, overheating of the ground compensates for the cooling of the sky during the day without cover, although the radiant temperature drops when there is no sun. However, the covered scenarios reduce the average radiant temperature by avoiding overheating the ground. The difference among scenarios are due to how the cover prevents overheating. The desired option bis the final scenario, as trees maintain a surface temperature slightly lower than the air temperature because of evapotranspiration.

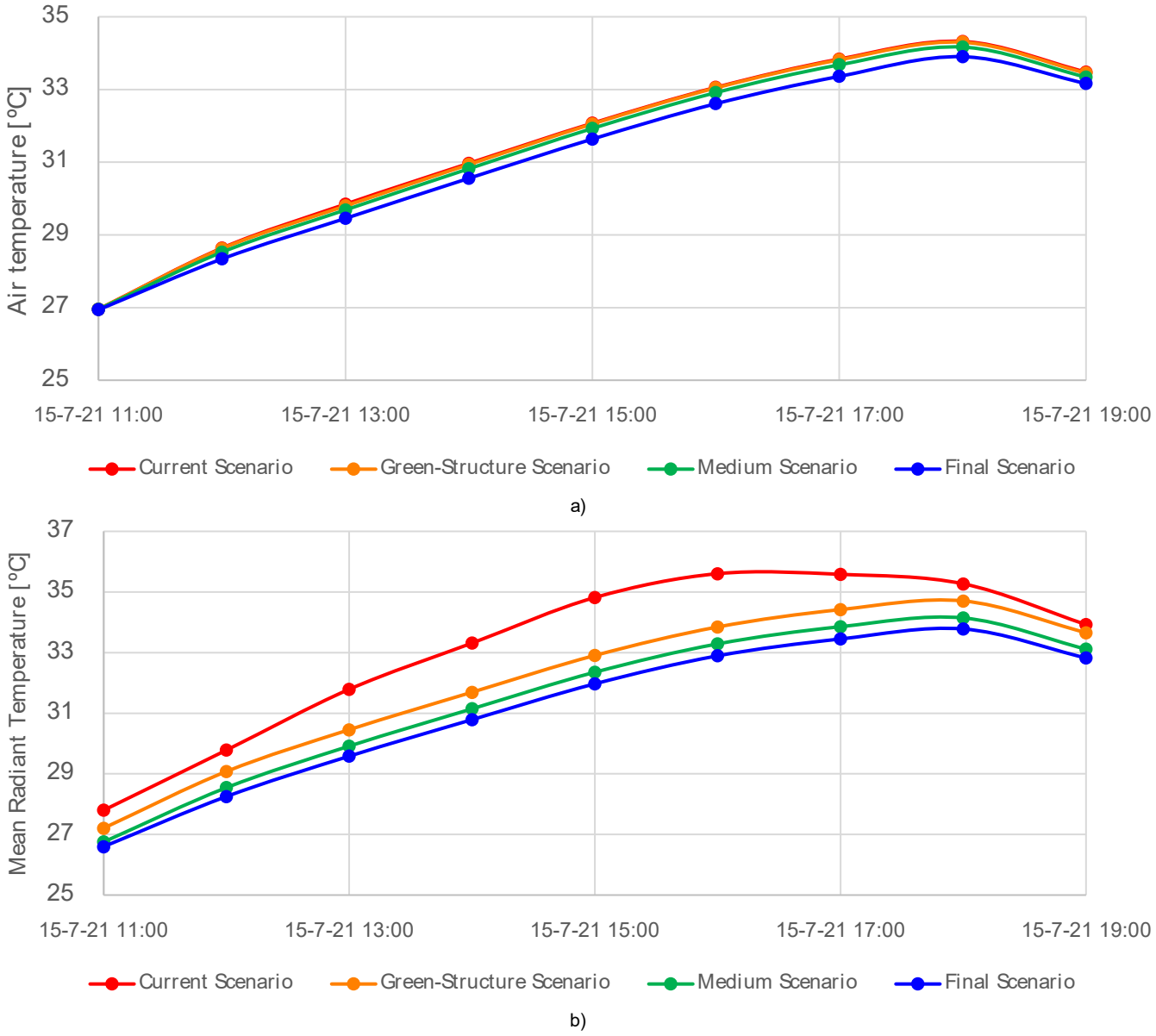

Figure 14. Mean air temperature (a) and mean radiant temperature (b) in the square on 15th July

3.1.2. Surface temperature

Regarding the surface temperatures, the differences obtained between the four scenarios were significant in both seasons. For 15th July at 12:00 h, the surface temperatures were 9 ºC lower in the areas where vegetation is incorporated, as shown in Figure 15a. The improvement obtained in the asphalted area, with temperatures 12 ºC lower, thanks to the vegetation, was noteworthy. In the scenarios involving the green

structure, the reduction in the surface temperature was slightly lower than that obtained with vegetation. Nevertheless, a space was created where the surface temperature was around 5ºC lower, despite not being completely covered with vegetation. For the same day at 18:00 h, the surface temperature was higher in the whole square, as shown in Figure 15b. Again, temperature differences were obtained of around 10 ºC, with a maximum of 12 ºC. In this case, the green structure led to a temperature decrease of 6 ºC, smaller than that achieved with vegetation. Finally, Figure 15c shows the variation in the surface temperature for 15th April at 12:00 h. In this case, the temperature difference between the current and the final scenario was around 10 ºC, with a maximum of 12 ºC in the asphalted area. In the medium scenario, the effect of the green structure was similar to that produced by vegetation.

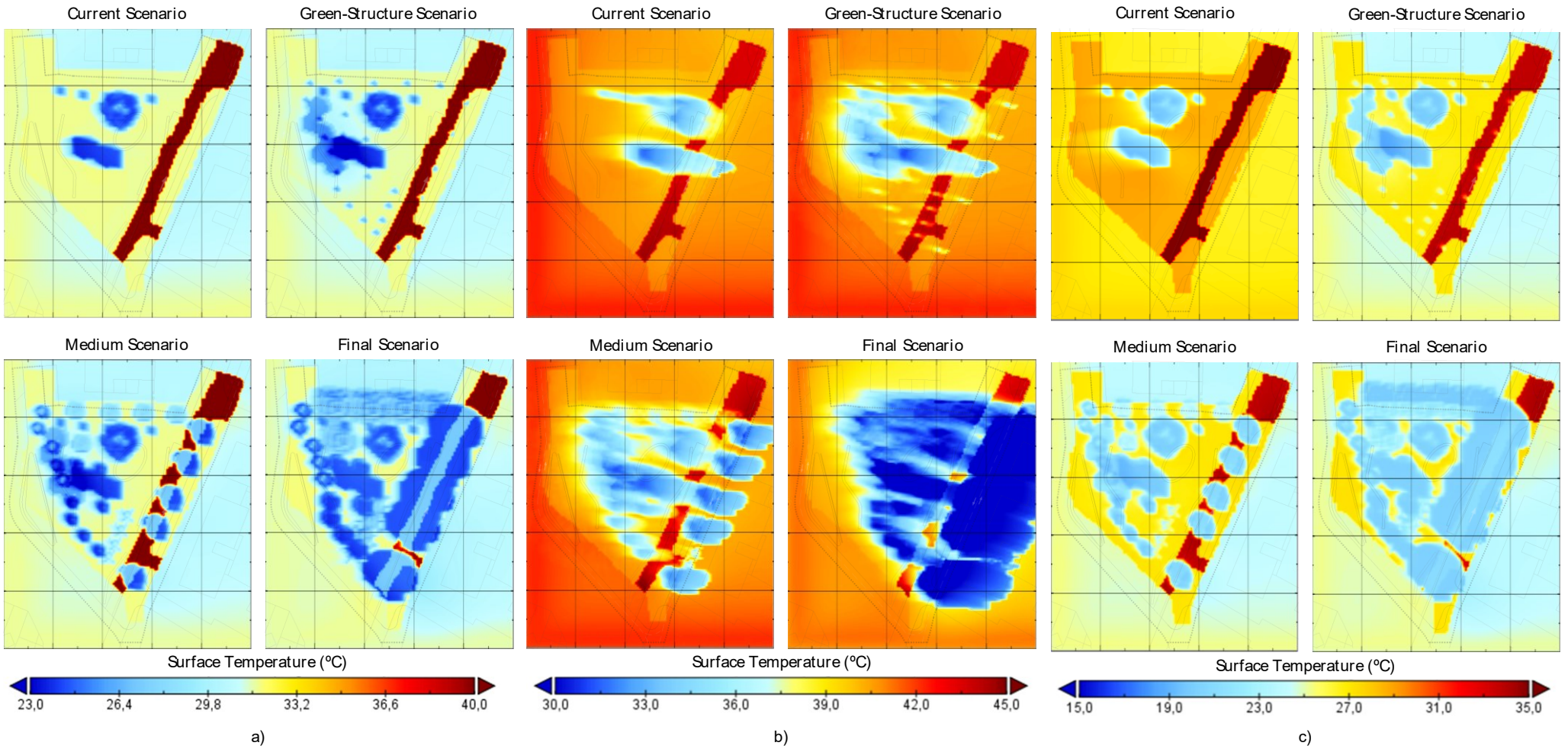

Figure 15. Surface temperatures in the four scenarios for 15th July at 12:00 (left), at 18:00 (centre) and for 15th April at 12:00 (right)

3.1.1. Incident radiation

In terms of radiation, the effect of the intervention in the square is striking. Figure 16a shows the results obtained from the simulation for 15th July at noon. The incident radiation in the square changed from 1000W/m^2 to practically zero in the final scenario. The green structure created a meeting point with 60% less radiation, improving livability from the start of the intervention. In addition, Figure 16b shows the effect achieved at 12:00 h on the spring day. The reduction was very similar to that obtained in the summer. The amount of radiation decreased until being non-existent in the areas with vegetation. In both summer and spring, the intervention in the square, with the incorporation of the green structure while the trees are growing, resulted in a city centre space with vastly improved climatic conditions during the whole year, enhancing the livability of the area.

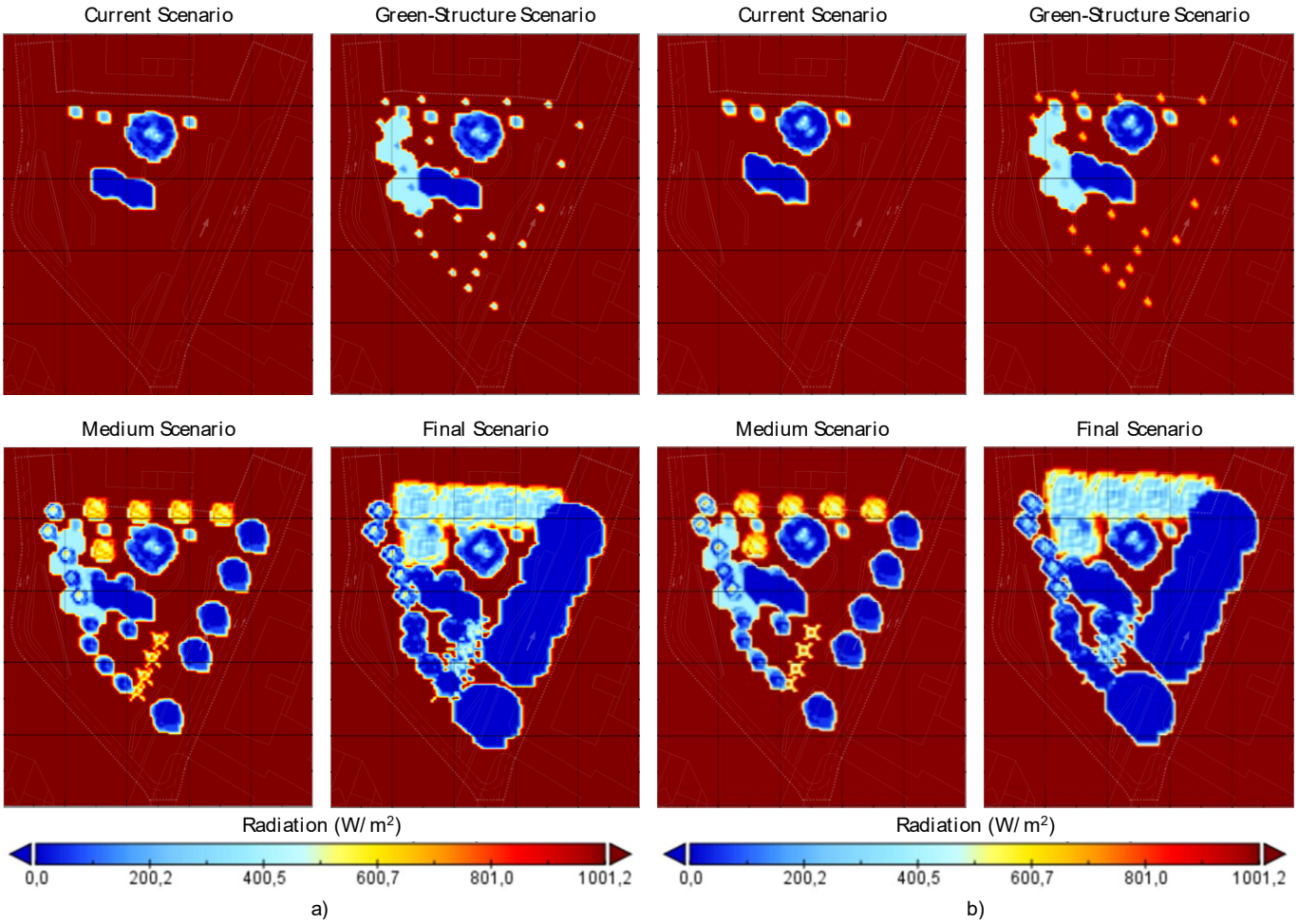

Figure 16. Incident radiation in the four scenarios for 15th July at 12:00 and for 15th April at 12:00

3.2. Comfort results

To determine the results in terms of comfort, the thermal load index of the COMFA model was assessed. The effect of the environmental conditions in this index was also analyzed for the two days studied. Currently, few structures in cities allow radiation to be blocked in summer. Figure 17 shows how the thermal stress indicator (Q [W/m^2]) of the COMFA method varies for the four scenarios studied. It can be noted that the proposed solution (Scenario 2, just after planting trees) manages to achieve a level of comfort equivalent to that which will finally be achieved with the trees in the square (Scenario 4, with the trees fully grown). These results justify the replicability of the solution as an urban prosthesis that adapts to the growth of trees. This would make it possible to enjoy regenerated urban areas with young vegetation from the very moment of intervention without having to wait 20 or 30 years for the trees to become adults.

On the other hand, the quantitative results of the thermal load and its evolution throughout the day can be compared according to the previously defined excitations, as well as the differences in the percentage of

the weight of the different heat flows discussed in section 3.3.4 on the thermal load at 2:00 p.m. local time, which has been taken as it is very close to solar noon. That is, when the sun is in its most unfavourable position from the point of view of thermal comfort in the street. Figure 17a shows the variation in the heat load for 15th July, as well as Figure 17b shows the variation in the heat load on 15th April. The positive values represent the heat load that the body of an occupant of the square needs to lose to be within the comfort zone. Conversely, the negative values imply the heat load their body needs to gain to be within the comfort zone. Regarding the current scenario for the 15th July, the mean heat load values required for a person to achieve comfort levels reached 200W/m^2 in the middle of the day, exceeding this value in three hours. It can be noted that thanks to this intervention, the loads were reduced by half (around 100W/m^2) at these times, even in the green structure scenario, where the heat load values decreased significantly compared with the current scenario.

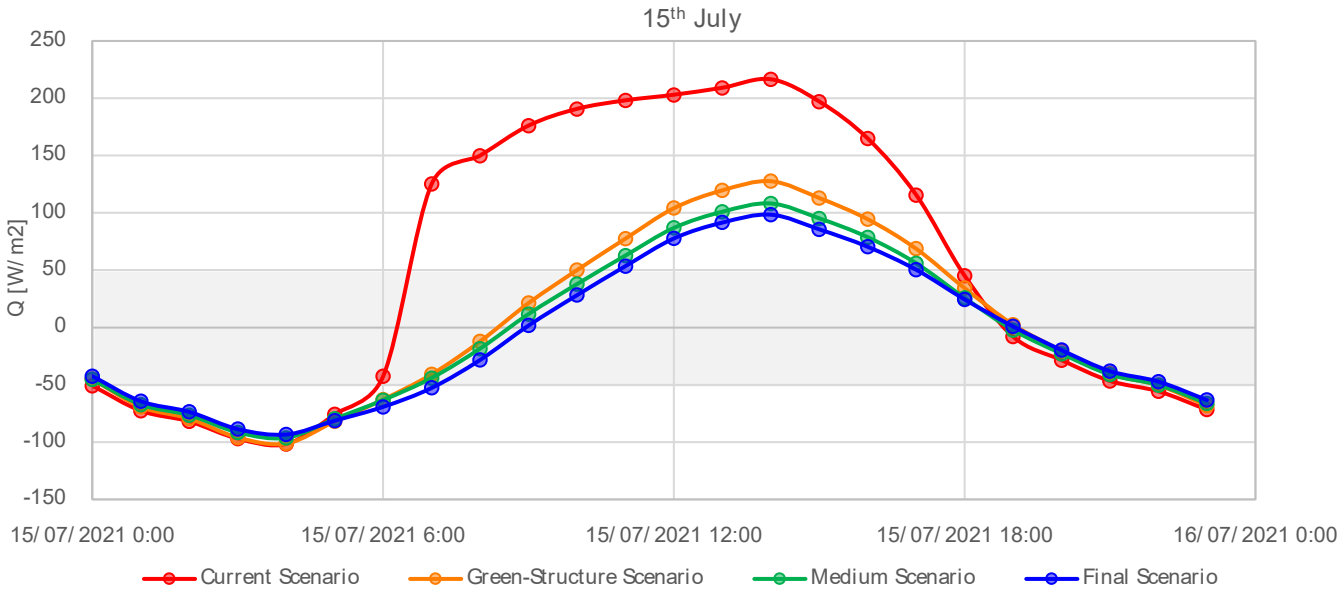

a)

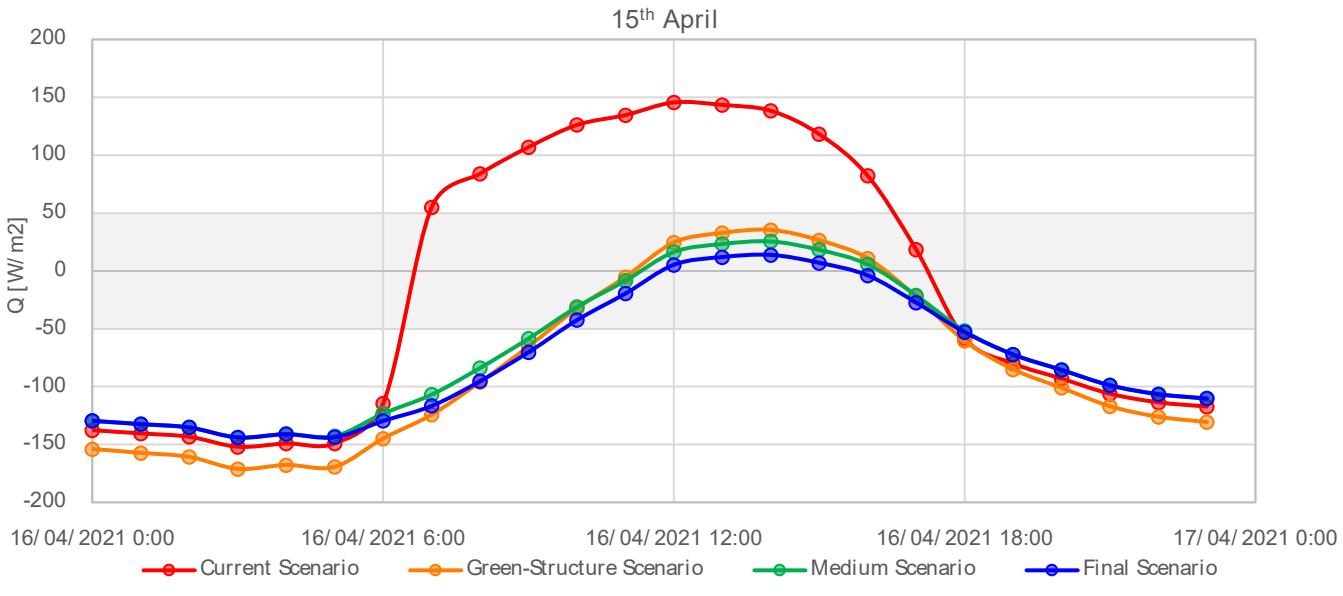

b)

Figure 17. Variation in heat load (summer (up) and spring (down))

Regarding the current scenario for the 15th April, the results were even more significant. The heat load in the current scenario (before renovation) reached around 150W/m^2. Since the time the trees are planted

(second and subsequent scenarios of the intervention), conditions of comfort were reached in the middle of the day, generating an open space with clearly improved conditions.

As mentioned above, several factors influence the heat load index: the person (metabolism, perspiration and breathing), direct radiation, diffuse radiation, and reflected radiation, in addition to convective air exchange and radiative exchange with the environment. For the same time, the person and the convective air exchange (which depends on win speed) remain constant in all four scenarios. Table 18 (left) shows the weight of each factor in the four scenarios for 12:00 h on 15th July, stressing that direct radiation becomes zero thanks to the intervention, as well as diffuse radiation and reflected radiation (which depends on the position of the occupant within the square) are also decreased. In the case of the effect produced by the radiative exchange, a heat gain can be observed as a result of the effect of the vegetation on surface and air temperatures in the square. It can be noted that the heat gained by a person from radiation was drastically reduced in the green structure scenario onwards. This highlights the positive effect of including a temporary artificial shading system in the summertime. Similarly, Table 18 (right) shows a breakdown of the factors affecting the heat load for 12:00 h on 15th April. Negative values from the start can be observed in radiative and convective exchanges. These results show that heat is dissipated from a person occupying the square. In addition, the drop in the air and surface temperatures, due to the inclusion of the vegetation in the final scenario, resulted in respective decreases in the thermal load of 32% (summer) and 21% (spring) regarding the current scenario.

Figure 18. Influence of heat load factors on thermal comfort (summer (left) and spring (right))

Heat Load Factor	Summer (15th July)				Spring (15th April)			
	1st *	2nd *	3rd *	4th *	1st *	2nd *	3rd *	4th *
Person (metabolism, perspiration and breathing)	82.3	82.3	82.3	82.3	80.5	80.5	80.5	80.5
Direct radiation	47.5	0.0	0.0	0.0	69.5	0.0	0.0	0.0
Diffuse radiation	48.4	6.9	4.3	0.9	45.9	4.7	4.1	0.8
Reflected radiation	12.5	7.4	5.8	0.9	11.8	6.4	5.4	0.8
Convective air exchange	-1.6	-1.6	-1.6	-1.6	-47.4	-47.4	-47.4	-47.4
Radiative exchange	13.9	9.2	-3.9	-4.7	-14.6	-16.7	-26.1	-29.5
Heat Load Index (sum of factors)	203.0	104.2	86.9	77.8	145.7	27.5	16.5	5.3

* 1st corresponds to the current scenario, 2nd corresponds to the green structure scenario, 3rd corresponds to the medium scenario and 4th corresponds to the final scenario

To sum up the analysis of results, Table 9 shows the number of hours in discomfort in the four scenarios for 15th July. In the current scenario, a person occupying the square experienced levels of discomfort for a total of 19 hours, decreasing to 13 hours in the final scenario. The integration of the temporary artificial solar shading reduced the number of hours in discomfort by 21%, while in the final scenario, this decrease was 32%. However, during the hours with the highest temperatures, a person cannot be in their comfort zone in the middle of the day. Therefore, other conditioning strategies are required to deal with the air or surface temperatures, which is a matter for future studies. Finally, a decrease in the number of hours in discomfort was also observed in the spring. In this case, thanks to the intervention, occupants managed to remain within their comfort zone during the day (10:00 h - 17:00 h) without requiring any additional action. The number of hours in discomfort was reduced by 32% after incorporating the adaptive shading, reducing the additional effect of the vegetation. It is important to note that there are still hours out of comfort, and the reduction in thermal stress is greater than 60%. Therefore, the indicator values of Q [W/m^2] are out of comfort, but it is possible to go from a current situation of suffocating to slightly hot. Different authors consider these new conditions as acceptable due to the thermal resilience of citizens (Li and Liu, 2020). Consequently, it supposes a good adaptation of the urban zone in front of the severe heat waves.

Table 9. Number of hours in discomfort during the studied days (summer and spring)

Scenario	Number of hours in discomfort

	Summer (15th July)	Spring (15th April)
Current Scenario	19	23
Green Structure Scenario	15	15
Medium scenario	13	13
Final Scenario	13	12

4. Conclusions

This study has designed and assessed a mitigation strategy for improving environmental conditions that consists of a temporary adaptive solar shading system solution combined with vegetation. The main aim is to improve the conditions of open spaces in urban areas with predominantly warm climates, as the case of Seville, from different standpoints, including climate. In this way, the thermal comfort can be ensured, health and well-being of the people using these spaces. There are many underused urban spaces with low or no solar control levels, which are impossible to use in the summer months in such urban climates. Therefore, the problem posed is a global concern that is the object of study by those responsible for the re-urbanization, regeneration and renovation of urban areas.

The solution combines vegetation with new urban elements, making the open space more livable. More vegetation is added to the square under study, covering almost the entire surface. To the best of our knowledge, there are no previous studies in the literature analyzing the effect of the progressive growth of trees. In this study, small trees were planted, which makes it impossible to obtain the desired level of shade at the time of planting. For this reason, an urban prosthesis has been designed and assessed for solar control that adapts to the growth of the trees, as well as to the seasons of the year. This solution was modelled according to real problems and characterized using on-site measurements. In addition, the system design facilitates its use in other urban areas when it is no longer required in the square under study. A numerical model was generated through ENVI-met to simulate the actual current situation and future scenarios, obtaining interesting results.

Increasing the vegetation results in a 0.5 ºC drop in the air temperature and a 12 ºC decrease in the surface temperature in the middle of the day in the year season with the highest temperatures. In months with intermediate temperatures, the reduction in the air temperature is 1ºC, while surface temperatures fall by up to 12ºC. In turn, radiation is drastically reduced thanks to the inclusion of vegetation in nearly 100% of the area.

Finally, thermal comfort was analyzed using the COMFA model using the heat load indicator (Q). When temperatures are high, the number of hours in discomfort is reduced by 21% when the adaptive solar shading is incorporated and by 30% when fully grown trees are considered. In addition, it is possible to convert 7% of the heat gain of the occupant thermal load due to surface temperatures into 6% dissipation. And most importantly, thermal stress, measured with the parameter of Q [W/m^2], is halved in the hottest hours of the day. However, it is worth highlighting that it is not possible to achieve levels of comfort during the middle of the day in the hottest months. This brings to light the need for action involving. For instance, combining mitigation strategies that use air treatment or changing surface materials. It can be noted that the results for the spring months are significant. The number of hours in discomfort is reduced by 30%, with levels of comfort being reached every hour of the day after incorporating the adaptive solar shading. In this case, the role of the greenery is reduced. The adaptive solar control system design is an effective means of counteracting the effects of climate change affecting urban areas, enabling it to be replicated in any urban area with a hot climate and providing to be reinstalled when the temporary artificial solution is no longer required in the initial intervention site. This strategy facilitates the design of green cities.

5. Acknowledgements

6. References

Alhusban, A.A., Alhusban, S.A., Alhusban, M.A., 2022. How the COVID 19 pandemic would change the

811 future of architectural design. J. Eng. Des. Technol. 20, 339–357. https://doi.org/10.1108/JEDT-03-
812 2021-0148
813 Angelotti, A., Dessì, V., Scudo, G., 2007. The evaluation of thermal comfort conditions in simplified urban
814 spaces : the COMFA + model. 2nd PALENC Conf. 1, 65–69.
815 Armson, D., Rahman, M.A., Ennos, A.R., 2013. A comparison of the shading effectiveness of five different
816 street tree species in Manchester, UK. Arboric. Urban For. 39, 157–164.
817 https://doi.org/10.48044/jauf.2013.021
818 ASHRAE, 2017a. ANSI/ASHRAE Standard 55: Thermal Environmental Conditions for Human
819 Occupancy.
820 ASHRAE, 2017b. ASHRAE Handbook Fundamentals - Chapter 8 Thermal Comfort, in: 2017 ASHRAE
821 Handbook Fundamentals. Atlanta.
822 ASHRAE, 2017c. ASHRAE fundamentals (SI), ASHRAE, "2017, ASHRAE fundamentals (SI)," in 2017,
823 ASHRAE fundamental handbook SI, 2017th.
824 Azcarate, I., Acero, J.Á., Garmendia, L., Rojí, E., 2021. Tree layout methodology for shading pedestrian
825 zones: Thermal comfort study in Bilbao (Northern Iberian Peninsula). Sustain. Cities Soc. 72.
826 https://doi.org/10.1016/j.scs.2021.102996
827 Blanco, M.J., Amieva, J.M., Mancillas, A., 2005. The Tonatiuh Software Development Project: An Open
828 Source Approach to the Simulation of Solar Concentrating Systems.
829 https://doi.org/10.1115/IMECE2005-81859
830 Blanco, M.J., Grigoriev, V., Milidonis, K., Tsouloupas, G., Larrañeta, M., Silva, M., 2021. Minimizing the
831 computational effort to optimize solar concentrators with the open-source tools sunpath and
832 tonatiuh++. Energies 14. https://doi.org/10.3390/en14154412
833 Brown, R.D., Gillespie, T.J., 1986. Estimating outdoor thermal comfort using a cylindrical radiation
834 thermometer and an energy budget model. Int. J. Biometeorol. 30, 43–52.
835 https://doi.org/10.1007/BF02192058
836 Bruse, M., 2018. ENVI-met. A holistic Microclimate Modelling System [A holistic microclimate model]
837 [WWW Document]. URL https://envi-met.info/doku.php?id=root:start (accessed 1.15.23).
838 Chatzinikolaou, E., Chalkias, C., Dimopoulou, E., 2018. Urban microclimate improvement using ENVI-
839 MET climate model. Int. Arch. Photogramm. Remote Sens. Spat. Inf. Sci. - ISPRS Arch. 42, 69–76.
840 https://doi.org/10.5194/isprs-archives-XLII-4-69-2018
841 Coccolo, S., Kämpf, J., Scartezzini, J.L., Pearlmutter, D., 2016. Outdoor human comfort and thermal stress:
842 A comprehensive review on models and standards. Urban Clim. 18, 33–57.
843 https://doi.org/10.1016/J.UCLIM.2016.08.004
844 Darvish, A., Eghbali, G., Eghbali, S.R., 2021. Tree-configuration and species effects on the indoor and
845 outdoor thermal condition and energy performance of courtyard buildings. Urban Clim. 37, 100861.
846 https://doi.org/10.1016/j.uclim.2021.100861
847 Degirmenci, K., Desouza, K.C., Fieuw, W., Watson, R.T., Yigitcanlar, T., 2021. Understanding policy and
848 technology responses in mitigating urban heat islands: A literature review and directions for future
849 research. Sustain. Cities Soc. 70, 102873. https://doi.org/10.1016/j.scs.2021.102873
850 Dimoudi, A., Nikolopoulou, M., 2003. Vegetation in the urban environment: Microclimatic analysis and
851 benefits. Energy Build. 35, 69–76. https://doi.org/10.1016/S0378-7788(02)00081-6
852 Du Bois, D., Du Bois, E.F., 1989. A formula to estimate the approximate surface area if height and weight
853 be known. 1916. Nutrition 5, 303.
854 Duan, X., He, C., Lin, X., Zhao, Y., Feng, J., 2020. Quasi-Monte Carlo ray tracing algorithm for radiative
855 flux distribution simulation. Sol. Energy 211, 167–182. https://doi.org/10.1016/j.solener.2020.09.061
856 Eisenhardt, K.M., Graebner, M.E., 2007. Theory building from cases: Opportunities and challenges. Acad.
857 Manag. J. 50, 25–32. https://doi.org/10.5465/amj.2007.24160888
858 El-Bardisy, W.M., Fahmy, M., El-Gohary, G.F., 2016. Climatic Sensitive Landscape Design: Towards a
859 Better Microclimate through Plantation in Public Schools, Cairo, Egypt. Procedia - Soc. Behav. Sci.
860 216, 206–216. https://doi.org/10.1016/j.sbspro.2015.12.029
861 Elgheznawy, D., Eltarabily, S., 2021. The impact of sun sail-shading strategy on the thermal comfort in
862 school courtyards, Building and Environment. Elsevier Ltd.
863 https://doi.org/10.1016/j.buildenv.2021.108046

Elnabawi, M.H., Hamza, N., Dudek, S., 2015. Numerical modelling evaluation for the microclimate of an outdoor urban form in Cairo, Egypt. HBRC J. 11, 246–251. https://doi.org/10.1016/j.hbrcj.2014.03.004

ENVI-met - Decode urban nature with ENVI-met software [WWW Document], n.d. URL https://www.envi-met.com/# (accessed 11.8.20).

Epstein, Y., Moran, D.S., 2006. Thermal comfort and the heat stress indices. Ind. Health 44, 388–398. https://doi.org/10.2486/indhealth.44.388

Escandón, R., Suárez, R., Sendra, J.J., 2019. Field assessment of thermal comfort conditions and energy performance of social housing: The case of hot summers in the Mediterranean climate. Energy Policy 128, 377–392. https://doi.org/10.1016/j.enpol.2019.01.009

Fabbri, K., Ugolini, A., Iacovella, A., Bianchi, A.P., 2020. The effect of vegetation in outdoor thermal comfort in archaeological area in urban context. Build. Environ. 175, 106816. https://doi.org/https://doi.org/10.1016/j.buildenv.2020.106816

Fahmy, M., Mahdy, M., Mahmoud, S., Abdelalim, M., Ezzeldin, S., Attia, S., 2020. Influence of urban canopy green coverage and future climate change scenarios on energy consumption of new sub-urban residential developments using coupled simulation techniques: A case study in Alexandria, Egypt. Energy Reports 6, 638–645. https://doi.org/10.1016/j.egyr.2019.09.042

Garcia-Nevado, E., Beckers, B., Coch, H., 2020. Assessing the Cooling Effect of Urban Textile Shading Devices Through Time-Lapse Thermography. Sustain. Cities Soc. 63, 102458. https://doi.org/10.1016/j.scs.2020.102458

Garreau, E., Berthou, T., Duplessis, B., Partenay, V., Marchio, D., 2021. Solar shading and multi-zone thermal simulation: Parsimonious modelling at urban scale. Energy Build. 249, 111176. https://doi.org/10.1016/j.enbuild.2021.111176

Garshasbi, S., Haddad, S., Paolini, R., Santamouris, M., Papangelis, G., Dandou, A., Methymaki, G., Portalakis, P., Tombrou, M., 2020. Urban mitigation and building adaptation to minimize the future cooling energy needs. Sol. Energy 204, 708–719. https://doi.org/10.1016/j.solener.2020.04.089

Georgi, J.N., Dimitriou, D., 2010. The contribution of urban green spaces to the improvement of environment in cities: Case study of Chania, Greece. Build. Environ. 45, 1401–1414. https://doi.org/10.1016/j.buildenv.2009.12.003

Guo, Z., Zhang, Z., Wu, X., Wang, J., Zhang, P., Ma, D., Liu, Y., 2020. Building shading affects the ecosystem service of urban green spaces: Carbon capture in street canyons. Ecol. Modell. 431, 109178. https://doi.org/10.1016/j.ecolmodel.2020.109178

Höppe, P., 2002. Different aspects of assessing indoor and outdoor thermal comfort. Energy Build. 34, 661–665. https://doi.org/10.1016/S0378-7788(02)00017-8

ISO, I.O. for S., 2005. ISO 7730 2005-11-15 Ergonomics of the Thermal Environment: Analytical Determination and Interpretation of Thermal Comfort Using Calculation of the PMV and PPD Indices and Local Thermal Comfort Criteria 0–2.

ISO, I.S.O., 2017. ISO 7243:2017 Index, Ergonomics of the thermal environment — Assessment of heat stress using the WBGT (wet bulb globe temperature).

Jafrancesco, D., Cardoso, J.P., Mutuberria, A., Leonardi, E., Les, I., Sansoni, P., Francini, F., Fontani, D., 2018. Optical simulation of a central receiver system: Comparison of different software tools. Renew. Sustain. Energy Rev. 94, 792–803. https://doi.org/10.1016/j.rser.2018.06.028

Jia, Y.P., Lu, K.F., Zheng, T., Li, X.B., Liu, X., Peng, Z.R., He, H. Di, 2021. Effects of roadside green infrastructure on particle exposure: A focus on cyclists and pedestrians on pathways between urban roads and vegetative barriers. Atmos. Pollut. Res. 12, 1–12. https://doi.org/10.1016/j.apr.2021.01.017

Johansson, E., Thorsson, S., Emmanuel, R., Krüger, E., 2014. Instruments and methods in outdoor thermal comfort studies – The need for standardization. Urban Clim. 10, 346–366. https://doi.org/10.1016/J.UCLIM.2013.12.002

Kántor, N., Chen, L., Gál, C. V., 2018. Human-biometeorological significance of shading in urban public spaces—Summertime measurements in Pécs, Hungary. Landsc. Urban Plan. 170, 241–255. https://doi.org/10.1016/j.landurbplan.2017.09.030

Kenny, N.A., Warland, J.S., Brown, R.D., Gillespie, T.G., 2009a. Part A: Assessing the performance of the comfa outdoor thermal comfort model on subjects performing physical activity. Int. J. Biometeorol.

53, 415–428. https://doi.org/10.1007/s00484-009-0226-3
Kenny, N.A., Warland, J.S., Brown, R.D., Gillespie, T.G., 2009b. Part B: Revisions to the COMFA outdoor thermal comfort model for application to subjects performing physical activity. Int. J. Biometeorol. 53, 429–441. https://doi.org/10.1007/s00484-009-0227-2
Kohler, M., Phillip, C.H., 2020. Outdoor thermal comfort acceptability calibration A calibration of the PET outdoor thermal comfort index in Singapore: does comfort vary respect to land uses? ETH Zurich Res. Collect. 1–40.
Kotharkar, R., Bagade, A., Singh, P.R., 2020. A systematic approach for urban heat island mitigation strategies in critical local climate zones of an Indian city. Urban Clim. 34, 1–17. https://doi.org/10.1016/j.uclim.2020.100701
Lai, D., Liu, W., Gan, T., Liu, K., Chen, Q., 2019. A review of mitigating strategies to improve the thermal environment and thermal comfort in urban outdoor spaces. Sci. Total Environ. 661, 337–353. https://doi.org/10.1016/j.scitotenv.2019.01.062
Lam, C.K.C., Weng, J., Liu, K., Hang, J., 2022. The effects of shading devices on outdoor thermal and visual comfort in Southern China during summer. Build. Environ. 228, 109743. https://doi.org/10.1016/j.buildenv.2022.109743
Lee, I., Voogt, J.A., Gillespie, T.J., 2018. Analysis and comparison of shading strategies to increase human thermal comfort in urban areas. Atmosphere (Basel). 9. https://doi.org/10.3390/atmos9030091
Li, J., Liu, N., 2020. The perception, optimization strategies and prospects of outdoor thermal comfort in China: A review. Build. Environ. 170, 106614. https://doi.org/10.1016/j.buildenv.2019.106614
Lindberg, F., Thorsson, S., Rayner, D., Lau, K., 2016. The impact of urban planning strategies on heat stress in a climate-change perspective. Sustain. Cities Soc. 25, 1–12. https://doi.org/10.1016/j.scs.2016.04.004
Mahmoud, A.H.A., 2011. Analysis of the microclimatic and human comfort conditions in an urban park in hot and arid regions. Build. Environ. 46, 2641–2656. https://doi.org/10.1016/j.buildenv.2011.06.025
Mehrotra, S., Subramanian, D., Bardhan, R., Jana, A., 2021. Effect of surface treatment and built form on thermal profile of open spaces: A case of Mumbai, India. Urban Clim. 35, 100736. https://doi.org/10.1016/j.uclim.2020.100736
Meili, N., Acero, J.A., Peleg, N., Manoli, G., Burlando, P., Fatichi, S., 2021. Vegetation cover and plant-trait effects on outdoor thermal comfort in a tropical city. Build. Environ. 195, 107733. https://doi.org/10.1016/j.buildenv.2021.107733
Montenon, A.C., Santos, A.V., Collares-Pereira, M., Montagnino, F.M., Garofalo, R., Papanicolas, C., 2022. Optical performance comparison of two receiver configurations for medium temperature Linear Fresnel Collectors. Sol. Energy 240, 225–236. https://doi.org/10.1016/j.solener.2022.05.029
NASA, 2022. Panoply nerCDF, HDF and GRIB Data Viewer [WWW Document].
Nasrollahi, N., Namazi, Y., Taleghani, M., 2021. The effect of urban shading and canyon geometry on outdoor thermal comfort in hot climates: A case study of Ahvaz, Iran. Sustain. Cities Soc. 65, 102638. https://doi.org/10.1016/j.scs.2020.102638
Nations, U., 2018. 68% of the world population projected to live in urban areas by 2050, says UN [WWW Document].
Nikolopoulou, M., Baker, N., Steemers, K., 2001. Thermal comfort in outdoor urban spaces: understanding the human parameter. Sol. Energy 70, 227–235. https://doi.org/10.1016/S0038-092X(00)00093-1
Nikolopoulou, M., Steemers, K., 2003. Thermal comfort and psychological adaptation as a guide for designing urban spaces. Energy Build. 35, 95–101. https://doi.org/10.1016/S0378-7788(02)00084-1
Ozarisoy, B., Altan, H., 2021. Regression forecasting of 'neutral' adaptive thermal comfort: A field study investigation in the south-eastern Mediterranean climate of Cyprus. Build. Environ. 202, 108013. https://doi.org/10.1016/j.buildenv.2021.108013
Park, Y., Guldmann, J.M., Liu, D., 2021. Impacts of tree and building shades on the urban heat island: Combining remote sensing, 3D digital city and spatial regression approaches. Comput. Environ. Urban Syst. 88, 101655. https://doi.org/10.1016/j.compenvurbsys.2021.101655
Pearlmutter, D., Jiao, D., Garb, Y., 2014. The relationship between bioclimatic thermal stress and subjective thermal sensation in pedestrian spaces. Int. J. Biometeorol. 58, 2111–2127. https://doi.org/10.1007/s00484-014-0812-x

970 Peel, M.C., Finlayson, B.L., McMahon, T.A., 2007. Updated world map of the Köppen-Geiger climate
971 classification. Hydrol. Earth Syst. Sci. 11, 1633–1644. https://doi.org/10.5194/hess-11-1633-2007
972 Peeters, A., Shashua-Bar, L., Meir, S., Shmulevich, R.R., Caspi, Y., Weyl, M., Motzafi-Haller, W., Angel,
973 N., 2020. A decision support tool for calculating effective shading in urban streets. Urban Clim. 34,
974 100672. https://doi.org/10.1016/j.uclim.2020.100672
975 Romero Rodríguez, L., Sánchez Ramos, J., Sánchez de la Flor, F.J., Álvarez Domínguez, S., 2020.
976 Analyzing the urban heat Island: Comprehensive methodology for data gathering and optimal design
977 of mobile transects. Sustain. Cities Soc. 55, 102027.
978 https://doi.org/https://doi.org/10.1016/j.scs.2020.102027
979 Rupp, R.F., Vásquez, N.G., Lamberts, R., 2015. A review of human thermal comfort in the built
980 environment. Energy Build. 105, 178–205. https://doi.org/10.1016/J.ENBUILD.2015.07.047
981 Sabrin, S., Karimi, M., Nazari, R., Pratt, J., Bryk, J., 2021. Effects of Different Urban-Vegetation
982 Morphology on the Canopy-level Thermal Comfort and the Cooling Benefits of Shade Trees: Case-
983 study in Philadelphia. Sustain. Cities Soc. 66, 102684. https://doi.org/10.1016/j.scs.2020.102684
984 Sánchez Ramos, J., Toulou, A., Guerrero Delgado, M., Palomo Amores, T.R., Castro Medina, D., Álvarez
985 Domínguez, S., 2022. Thermal Resilience of Citizens: Comparison between Thermal Sensation and
986 Objective Estimation in Outdoor Spaces: A Case Study in Seville, Spain. Appl. Sci. 12.
987 https://doi.org/10.3390/app122211676
988 Sharmin, T., Steemers, K., 2016. Responsiveness of Microclimate Simulation Tool in Recognising
989 Diversity in Urban Geometry.
990 Sharmin, T., Steemers, K., 2015. Use of Microclimate Models for Evaluating Thermal Comfort: Identifying
991 the Gaps.
992 Standard, I.I.S.O., 2004. ISO 7933:2004 Ergonomics of the thermal environment — Analytical
993 determination and interpretation of heat stress using calculation of the predicted heat strain.
994 Stocco, S., Cantón, M.A., Correa, E.N., 2015. Design of urban green square in dry areas: Thermal
995 performance and comfort. Urban For. Urban Green. 14, 323–335.
996 https://doi.org/10.1016/j.ufug.2015.03.001
997 Takakura, T., Jordan, K.A., Boyd, L.L., 1971. Dynamic Simulation of Plant Growth and Environment in
998 the Greenhouse. Trans. ASAE 14, 0964–0971. https://doi.org/10.13031/2013.38432
999 Thomas, G., Thomas, J., Mathews, G.M., Alexander, S.P., Jose, J., 2023. Assessment of the potential of
1000 green wall on modification of local urban microclimate in humid tropical climate using ENVI-met
1001 model. Ecol. Eng. 187, 106868. https://doi.org/10.1016/j.ecoleng.2022.106868
1002 Thomson, H., Simcock, N., Bouzarovski, S., Petrova, S., 2019. Energy poverty and indoor cooling: An
1003 overlooked issue in Europe. Energy Build. 196, 21–29. https://doi.org/10.1016/j.enbuild.2019.05.014
1004 Unal Cilek, M., Uslu, C., 2022. Modeling the relationship between the geometric characteristics of urban
1005 green spaces and thermal comfort: The case of Adana city. Sustain. Cities Soc. 79, 103748.
1006 https://doi.org/10.1016/j.scs.2022.103748
1007 Upreti, R., Wang, Z.H., Yang, J., 2017. Radiative shading effect of urban trees on cooling the regional built
1008 environment. Urban For. Urban Green. 26, 18–24. https://doi.org/10.1016/j.ufug.2017.05.008
1009 Vanos, J.K., Warland, J.S., Gillespie, T.J., Kenny, N.A., 2012. Thermal comfort modelling of body
1010 temperature and psychological variations of a human exercising in an outdoor environment. Int. J.
1011 Biometeorol. 56, 21–32. https://doi.org/10.1007/s00484-010-0393-2
1012 Watanabe, S., Nagano, K., Ishii, J., Horikoshi, T., 2014. Evaluation of outdoor thermal comfort in sunlight,
1013 building shade, and pergola shade during summer in a humid subtropical region. Build. Environ. 82,
1014 556–565. https://doi.org/10.1016/j.buildenv.2014.10.002
1015 Yin, R.K., 2013. Case study research: Design and methods, 5th ed. SAGE Publications, Thousand Oaks,
1016 CA, USA.
1017 Yin, S., Wang, F., Xiao, Y., Xue, S., 2022. Comparing cooling efficiency of shading strategies for
1018 pedestrian thermal comfort in street canyons of traditional shophouse neighbourhoods in Guangzhou,
1019 China. Urban Clim. 43, 101165. https://doi.org/10.1016/j.uclim.2022.101165
1020 Zabetian, E., Kheyroddin, R., 2019. Comparative evaluation of relationship between psychological
1021 adaptations in order to reach thermal comfort and sense of place in urban spaces. Urban Clim. 29,
1022 100483. https://doi.org/10.1016/j.uclim.2019.100483

Zeeshan, M., Ali, Z., Ud Din, E., 2022. Thermal performance prediction of street trees inside isolated open spaces–evaluations from real scale retrofitting project. J. Build. Perform. Simul. https://doi.org/10.1080/19401493.2022.2038270

Zhu, S., Causone, F., Gao, N., Ye, Y., Jin, X., Zhou, X., Shi, X., 2023. Numerical simulation to assess the impact of urban green infrastructure on building energy use: A review. Build. Environ. 228. https://doi.org/10.1016/j.buildenv.2022.109832